Aus dem Neurowissenschaftlichen Forschungszentrum
der Medizinischen Fakultät Charité – Universitätsmedizin Berlin

DISSERTATION

Investigation of striatal GABAergic output modulation by glutamatergic input

zur Erlangung des akademischen Grades
Doctor of Philosophy (PhD)
im Rahmen des
International Graduate Program Medical Neurosciences

vorgelegt der Medizinischen Fakultät
Charité – Universitätsmedizin Berlin

von

Foteini Paraskevopoulou
aus Athen, Griechenland

Datum der Promotion:

4. Juni 2021

Contents

Abstract

Maintaining the balance between excitation and inhibition within neural circuits is crucial to healthy brain function. Glutamatergic inputs from the cortex and thalamus onto neurons in the striatum seem to play a central role in the development of goal-directed behaviors, including movement and cognition. However, the exact mechanisms through which glutamatergic inputs modulate striatal neurons' output are still unknown. In this study, we performed in-depth electrophysiological and morphological assays in primary cultured mouse neurons to investigate the role of glutamatergic innervation in striatal GABAergic transmission. Using a two-neuron microcircuit culture model, in which each neuron forms synaptic connections onto itself (autapses) as well as onto the partner neuron (heterosynapses), we could study the interaction of only two neurons of known identity and tissue origin and assess the synaptic properties of all possible connections. By comparing the release characteristics of striatal GABAergic neurons partnered with either a cortical or thalamic glutamatergic neuron or with another striatal GABAergic neuron, we found that glutamatergic input of both origins enhances GABAergic synaptic transmission. In particular, cortical and thalamic innervation causes an increase in the strength of GABAergic responses on striatal neurons. However, increase in the number of readily releasable GABAergic synaptic vesicles and morphological synapses was only induced by cortical innervation. These alterations were contingent on action potential generation, glutamatergic synaptic transmission and BDNF secretion. As cortico-striatal and thalamo-striatal circuits are involved in several neurological diseases, such as Huntington's disease and psychiatric disorders, our findings may contribute to better understand the pathophysiology of such diseases.

Zusammenfassung

Die Aufrechterhaltung des Gleichgewichts zwischen Erregung und Hemmung in neuronalen Schaltkreisen ist für eine gesunde Gehirnfunktion entscheidend. Kortikale und thalamische glutamaterge Innervation auf Neuronen im Striatum, scheinen eine zentrale Rolle bei der Entwicklung von zielgerichtetem Verhalten zu spielen. Die genauen Mechanismen, durch die glutamatergische Innervationen striatale Neuronen modulieren können, sind jedoch noch unbekannt. In dieser Studie werden detaillierte elektrophysiologische und morphologische Untersuchungen in primär kultivierten Mausneuronen durchgeführt, um die Rolle der glutamatergen Innervation bei der striatalen GABAergen Übertragung zu untersuchen. Mit Hilfe eines Zwei-Neuronen-Zellkulturmodells, bei dem jedes Neuron synaptische Verbindungen sowohl zu sich selbst (Autapsen) als auch zu einem Partner-Neuron (Heterosynapsen) eingeht, wurden die Beziehungen von nur zwei Neuronen mit bekannter Identität und Gewebsursprung untersucht, und die synaptische Eigenschaften aller auftretenden Verbindungen bewertet. Der Vergleich der Neurotransmitter Freisetzungseigenschaften von striatalen GABAergen Neuronen, die sich entweder mit einem kortikalen oder thalamischen glutamatergen Neuron oder mit einem anderen striatalen GABAergen Neuron entwickelt haben, zeigte, dass der glutamaterge Eingang beider Ursprünge die GABAerge synaptische Übertragung verbessert. Insbesondere die kortikale und thalamische Innervation bewirkt eine Erhöhung der Stärke der GABAergen Reaktion auf striatale Neuronen. Die Zunahme der Anzahl der leicht freisetzbaren GABAergen synaptischen Vesikel und der Anzahl von morphologischen Synapsen wurde jedoch nur durch kortikale Innervation induziert. Diese Änderungen waren abhängig von der Erzeugung des Aktionspotenzials, der glutamatergen synaptischen Übertragung und der BDNF-Sekretion. Da kortiko-striatale und thalamo-striatale Kreisläufe an mehreren neurologischen Erkrankungen wie Huntington-Krankheit und psychiatrischen Erkrankungen beteiligt sind, können unsere Erkenntnisse dazu beitragen, die Pathophysiologie solcher Erkrankungen besser zu verstehen.

1. Introduction

Chemical synapses are the key connective elements in neuronal networks and are crucial for information processing and transmission. Neuronal circuits are composed of mainly excitatory glutamatergic and inhibitory GABAergic neurons, which communicate through synaptic connections. Balanced excitation and inhibition is a crucial feature of a healthy neural network (Chagnac-Amitai and Connors, 1989). In fact, disruption of the excitation/inhibition balance prevents normal neural circuit function (Ramamoorthi and Lin, 2011) and is hypothesized to be the root of many neurological disorders, including autism or Huntington's disease (Graybiel, 2000; Nelson and Valakh, 2015). At first glance, one would think that a cell's self-regulatory mechanisms are sufficient to control the process of neurotransmission and thus, the functional balance between excitatory and inhibitory synapses. However, accumulating evidence and studies have proven that the reality is more complicated than previously thought. Neurons interact with each other in networks and receive synaptic inputs in response to alterations in neuronal activity. Particularly vulnerable in this process are the GABAergic neurons (Hartman et al., 2006; Huang, 2009). Inhibition via GABAergic synapses plays an instructional role at regulating the network excitability. Therefore, understanding the mechanisms underlying the regulation of both GABAergic synapse number and function is important for striving to restore balance in disrupted states.

Neuronal activity is a strong candidate to regulate the formation and function of GABAergic synapses (Chattopadhyaya et al., 2004; Hartman et al., 2006). A number of studies have shown that chronic blockade of neuronal activity in dissociated cultures of neocortex, triggers a reduction in the amount of inhibition (Marty et al., 1996; Rutherford et al., 1997; Kilman et al., 2002). To add on, Hartman et al. (2006) showed that changes in the activity of individual hippocampal neurons are not sufficient to cause reduction of GABAergic synapses, whereas alterations in the levels of overall network activity promotes changes in GABAergic synapse density. Similarly, in slice cultures of cerebellum and hippocampus, activity blockade with TTX reversibly decreases GABA immunoreactivity and modulates the number of inhibitory synapses received by cultured Purkinje (Seil and Drake-Baumann, 1994, 2000) and hippocampal neurons (Marty et al., 2000). Altogether, these studies prove that neuronal activity is able to adjust the strength of synaptic inhibition, but the exact mechanism underlying these processes remain elusive.

A potential signal linking activity to the modulation of synaptic inhibition is the neurotrophin, brain-derived neurotrophic factor (BDNF). BDNF is synthesized and released by pyramidal cells in an activity-dependent manner (Thoenen, 1995) and it has been suggested to

promote formation of GABAergic synapses in hippocampal and cortical cultures (Rutherford et al., 1997; Vicario-abejo et al., 1998; Brünig et al., 2001). Specifically, by regulating neuronal morphology or stabilization of the cellular and molecular components that are responsible for neurotransmitter release, BDNF release leads to an increase in the number of functional inhibitory synapses (reviewed in Vicario-abejón et al., 2002). Previous studies in interneurons propose that BDNF not only functions as an activity-dependent, autocrine, retrograde messenger in excitatory cells, but also has paracrine action in interneurons (Marty et al., 1996). In this way, the levels of BDNF release from adjacent cells regulate hippocampal inhibition. Whether the same mechanism of activity-dependent BDNF release is responsible for modulation of inhibitory output in other populations of GABAergic neurons, such as projection neurons, as well as the exact sites of modification are still not defined.

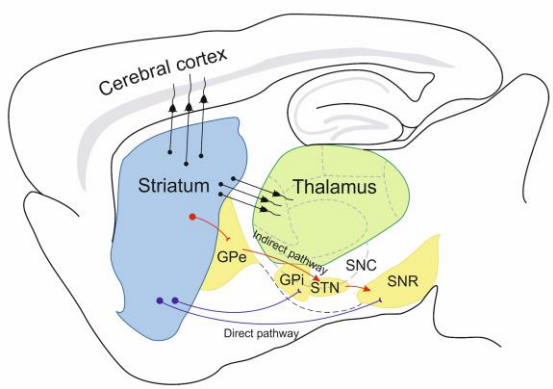

Figure 1. Schematic diagram (redrawn after Surmeier et al., 2007) showing anatomical connections of striatum in mouse brain. Abbreviations: GPe, globus pallidus external; GPi, globus pallidus internal; STN, subthalamic nucleus; SNC, substantia nigra pars compacta; SNR, substantia nigra pars reticulate.

The striatum is an ideal model to investigate the formation and function of inhibitory synapses, since it is a structure rich in GABAergic neurons and, especially, projection neurons (Figure 1). Medium spiny neurons (MSNs) make up the principle population representing ~95% of striatal neurons and are morphologically homogeneous. Based on their downstream projection targets and the type of dopamine receptor they express (D1 or D2), MSNs are classified into two major categories that control movement in opposing ways: the D1-MSNs of the direct pathway facilitate movement, and the D2-MSNs of the indirect pathway suppress movement (Albin et al., 1989; Gerfen, 1992). Direct pathway MSNs send their axons to globus pallidus internal (GPi) and substantia nigra pars reticulata (SNR), while indirect pathway MSNs project first to globus pallidus external (GPe) and subthalamic nucleus (STN) (Albin et al., 1989; DeLong, 1990). Both types of MSNs receive massive excitatory input from glutamatergic neurons originating from neocortex or

specific thalamic nuclei (Kreitzer and Malenka, 2008). Cortical efferents form asymmetric synapses onto striatal dendritic spines and convey motor-related information (Gerfen, 1984; Wilson, 2014). In addition, thalamostriatal projections form synaptic contacts on the dendritic shafts of striatal MSNs and in this way impact the processing of functionally segregated information (Smith et al., 2004).

Since striatal neurons are mainly GABAergic and their only source of excitation and BDNF comes from glutamatergic input, the latter might function as a possible component for shaping the output of striatal neurons. Chang et al. (2014) revealed that glutamatergic input in the hippocampus regulates inhibitory output of interneurons, through control of synaptic vesicle release efficiency and synapse formation. However, there has been no attempt to-date to directly explore how cortico- and thalamo-striatal pathways modulate striatal circuit activity. *In vivo* studies on intracellular recordings of behaving animals and striatal slices (Wilson, 1993; Ding et al., 2008) have shown that changes in cortical activity can be followed by shifts in striatal depolarization states in a stereotyped fashion (Stern et al., 1997). Although these studies provide significant knowledge, it is now accepted that to directly dissect the properties of cortico-striatal or thalamo-striatal connections, *in vitro* dissociated cell culture systems that allow for the identification of single pairs and individual neuron inputs and outputs of striatal neurons are required (Randall et al., 2011). Recording pairs of connected neurons in a simplified system allows for the evaluation of the number of synaptic contacts involved in striatal transmission and identification of the synaptic properties of all the possible connections. Furthermore, distinct components of glutamatergic innervation, such as activity or release of brain derived neurotrophic factor (BDNF) can be explored separately in this configuration.

1.1. Objectives of the project

In the present thesis project, we examined the molecular mechanisms affecting formation and function of inhibitory synapses in striatal neurons in the presence of glutamatergic innervation. To achieve this, we used an *in vitro* dissociated two-neuron inter-regional microcircuit and carried out paired whole cell patch clamp recordings (455 pairs). To complement the findings of electrophysiological experiments, we also performed immunocytochemistry and quantified the number of inhibitory synapses in the two-neuron configuration (191 pairs). Frist, we explored whether the effects of cortico-striatal connections differ from those of thalamo-striatal. We found that either glutamatergic input onto striatal GABAergic neurons enhanced inhibitory synaptic transmission by regulating their output, but only the cortical partner was able to promote formation

of more synapses. Second, we examined the contribution of individual glutamatergic innervation components on GABAergic synapse formation and function (Hartman et al., 2006; Park and Poo, 2013; Chang et al., 2014). In this respect, we i) investigated the role of activity and glutamatergic firing and ii) examined the effect of BDNF release from cortical neurons onto striatal GABAergic synapse function. We revealed that cortical-induced changes in striatal neuron output were dependent on action potential generation, glutamatergic synaptic transmission and BDNF secretion. Chronically blocking Trk receptors with an antagonist or blocking BDNF function with an anti-BDNF neutralization antibody resulted in a decrease of striatal synaptic output and synapse number. Together, our results provide novel insights into basal ganglia physiology and suggest that two-neuron *in vitro* microcircuits could be a powerful tool to explore synaptic mechanisms or disease pathophysiology.

2. Materials and Methods

2.1. Mice

All experiments have been conducted in full compliance with the guidelines for animals handling and have been approved by the Animal Welfare Committee of Charité Medical University and the Berlin State Government Agency for Health and Social Services (License T0220/09). Newborn C57BLJ6/N mice at postnatal (P) day 0-2 of both sexes were used for all the experiments involving electrophysiological and morphological assays.

2.2. Cell culture

2.2.1 Two-neuron microcircuits

To prepare the desired substrate for our neuronal cultures, 2 weeks before the neuronal preparation, sterilized and alkaline treated coverslips were coated with 0.15% agarose. Subsequently, coverslips were coated with a substrate mixture of 17 mM acetic acid, 4 mg/ml collagen and 0.5 mg/ml poly-D-lysine using a custom rubber stamp and allowing astrocytes to grow only in dots ("microislands"). The resulted astrocytic microislands had a uniform diameter of 200µm. Astrocytes were derived from C57BL6/N mouse cortices (P0-1) after dissociation of the tissue and plated at a density of 50,000 cells per 35 mm.

For neuronal cultures, preferred tissues (striatum, cortex or thalamus) were dissected in ice-cold HBSS and were digested with 25 U/ml papain in DMEM (Worthington) at 37^{o}C for 45 min. Following incubation, papain was inactivated by a pre-warmed solution of albumin, trypsin

inhibitor, and 5% fetal calf serum (FCS) for 5 min. The inactivation solution was then removed and Neurobasal-A (NBA) media containing B-27 supplement and Glutamax (Invitrogen), 50 IU/ml penicillin and 50 μg/ml streptomycin, was added to the tissue that was triturated several times by repeated pipetting. Neurons were mechanically dissociated and plated on astrocytic islands in supplemented NBA media. For two-neuron heterotypic (cortico-striatal or thalamo-striatal pairs) cultures, neurons were plated at 1:1 ratio and at a total density of $1x10^4$ neurons per 35 mm well. For control (homotypic; striatal-striatal) pairs, neurons were plated at final density 5,000 cells per 35 mm. For autaptic cultures (single neuron per microisland), neurons were plated at density 4,000 cells per 35 mm. Under this conditions, neurons on isolated microislands formed recurrent synapses, also referred to as "autapses" (Bekkers and Stevens, 1991) and heterosynaptic connections with their partner. Neurons were incubated at 37 °C for 12–15 days to grow in supplemented NBA media, before initiating the experiments.

2.2.2 Membrane dye labeling

To identify the neurons' region of origin in electrophysiological recordings, neurons from each brain region were labeled with different fluorescent membrane dyes (PKH26 red or PKH67 green), using a fluorescent cell linker kit for general membrane labeling (Sigma). According to the manufacturer's protocol, dissociated cells were centrifuged at 1700 rpm for 6 min. Supernatant was replaced with dye solution and cell pellet was suspended by gentle pipetting. Following 5 min incubation, staining reaction was halted by a pre-warmed solution of FCS for 1 min. Subsequently, the serum solution was removed and Neurobasal-A (NBA) media containing B-27 supplement and Glutamax (Invitrogen), 50 IU/ml penicillin and 50 μg/ml streptomycin was added to cells and resuspended by repeated pipetting. In the next step, neurons from different tissues (cortex, thalamus, striatum) were mixed in 1:1 ratio and seeded on astrocytic microislands. This procedure enabled identification of homotypic (striatal) and heterotypic (cortico- striatalor thalamo-striatal) pairs of known origin.

2.2.3 Drug treatments

To investigate the contribution of individual gluatamtergic innervation components on striatal GABAergic synapse formation and function, we treated cultures with the following drugs: i) human recombinant BDNF (50 ng/ml; Peprotech); ii) highly selective and reversible sodium channel blocker tetrodotoxin (0.5 μM TTX; Tocris Bioscience); iii) selective and competitive AMPA receptor antagonist 2,3-dihydroxy-6-nitro-7-sulfamoyl-benzo[f]quinoxaline-2,3-dione (2 μM NBQX; Tocris Bioscience) and NMDA receptor antagonist d-(-)-2-amino-5-

phosphonopentanoic acid (100 μM APV; Tocris Bioscience); iv) non-selecitive protein kinase inhibitor K252a (200 nM; Tocris Bioscience) and v) BDNF neutralizing antibody α-BDNF (1:100; Millipore) at days *in vitro* (DIV) 3, 7, 11.

2.3. Electrophysiology

Synaptic function of autaptic striatal neurons or homotypic and heterotypic pairs was measured by whole-cell voltage-clamp recordings between days *in vitro* (DIV) 12–15. In paired recordings using our microisland culture system, one cell at a time was stimulated and synaptic responses in both cells were measured (Figure 2; detailed methodological scheme). Postsynaptic currents were recorded with the use of a Multiclamp 700B amplifier (Molecular Devices, Sunnyvale, CA) and Axon Digidata 1440A digitizer (Molecular Devices) under the control of Clampex 10.2 (Molecular Devices). Neurons were held at -70 mV (holding potential) and series resistance was compensated by 70%. Only cells with less than 12 MΩ series resistance were analyzed. Data were acquired using at 10 kHz and low-pass Bessel filtered at 3 kHz. All experiments were performed blinded, at room temperature (RT; 23–24°C) and data from at least three independent cultures were analyzed per experiment. To account for systematic errors, coverslips were always randomized to drug treatments in all experiments.

During recordings, neurons were immersed in standard extracellular solution consisting of (in mM): 140 NaCl, 2.4 KCl, 10 HEPES, 10 glucose, 4 $MgCl_2$, and 2 $CaCl_2$. Borosilicate glass patch pipettes of 2-3.5 MΩ resistance were pulled with a multistep puller (P-87, Sutter Instruments) and filled with internal solution contained the following (in mM): 136 KCl, 17.8 HEPES, 1 EGTA, 0.6 $MgCl_2$, 4 ATP-Mg, 0.3 GTP-Na, 12 phosphocreatine, and 50 U/ml phosphocreatine kinase. Both solutions were adjusted to pH 7.4 with osmolarity at 300 mOsm. Action potential evoked postsynaptic currents (PSCs) were triggered by a 2 ms somatic depolarization from -70 mV (holding potential) to 0 mV. After stimulating neurons at 0.1 Hz in standard external solution, evoked excitatory or inhibitory postsynaptic currents (EPSCs or IPSCs, respectively) were measured. The excitatory or inhibitory identity of the neurons was verified by the kinetics of the evoked responses and AMPA receptor antagonist (3 μM 2,3-dihydroxy-6-nitro-7-sulfamoyl-benzo[f]quinoxaline-2,3-dione (NBQX); Tocris Bioscience) or GABAA receptor antagonist (30 μM bicuculine; Tocris Bioscience). To determine the spontaneous release of GABAergic cells, miniature IPSCs (mIPSCs) were recorded at −70 mV in the presence of extracellular solution with NBQX and for a time period of 20–40 s. Analysis of mIPSC was performed using a template-based algorithm as implemented in Axograph X v1.6.4. Specifically,

data were filtered at 1kHz and the threshold for detection was set at three times the baseline SD from a template of 0.5 ms rise time and 18 ms decay time for GABAergic events. Membrane capacitance measurements were obtained from the membrane test function in pClamp (Molecular Devices). Readily releasable pool (RRP) size of striatal cells (GABAergic only) was assessed by measuring the charge transfer of the transient synaptic current induced by a 5 s application of 500 mM hypertonic sucrose (Rosenmund et al., 1996) in standard extracellular solution supplemented with NBQX. Application of sucrose/NBQX solution resulted in a transient inward current (duration 2-3 s) that represent RRP release itself and a steady-state current that denotes the point when the rates of synaptic vesicle pool refilling and release are equal. In heterotypic pairs (Glu-GABA), the output RRP was the sum of the autaptic and heterosynaptic transient RRP currents. Conversely, in striatal pairs, where the individual GABAergic RRP sucrose-induced currents cannot be distinguished, the total RRP was equally divided between the two neurons (Figure 2C). For estimating the number of RRP synaptic vesicles the sucrose charge was divided by the charge of the average miniature event of the same neuron. The release probability of a single synapse (Pvr) was determined dividing the input evoked response charge (autaptic and heterosynaptic connections ending at each postsynaptic neuron) by the RRP charge within a neuron. Finally, the paired-pulse ratio (PPR; response 2/ response 1) was calculated by evoking 2 responses with an inter-stimulus interval of 50 ms (Figure 2B).

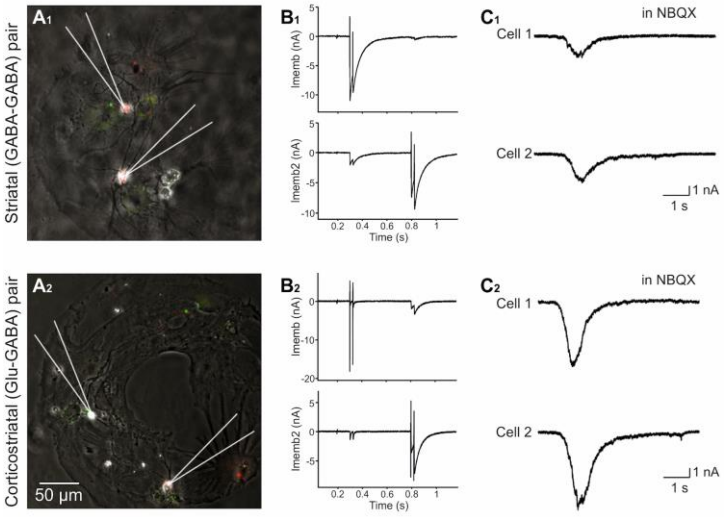

Figure 2: In voltage-clamp paired recordings, the induction of an action potential in a neuron results in postsynaptic response onto itself (autaptic response) and onto its partner neuron (heterosynaptic response). In microisland preparation, this leads to the stimulation of two out of four synapse formed. The other two synapses are stimulated when the second neuron gets an action potential. In these recording conditions one cell is stimulated consequently the other after approximately 500 ms. This stimulation pattern gets repeated five times for each pair. (A) Representative images of striatal and cortico-striatal pairs labeled with fluorescent membrane dyes. (B-C) Representative traces of paired whole-cell voltage-clamp recordings. (B) Evoked synaptic responses (EPSCs or IPSCs) after application of PPR (50ms ISI). (C) Readily releasable pool (RRP) size of striatal cells (GABAergic only) induced by 500 mM sucrose in standard extracellular solution supplemented with NBQX.

All analyses were performed in Axograph X (Axograph Scientific, Berkeley, CA), Excel (Microsoft, Redmond, WA) and Prism (GraphPad, La Jolla, CA). Neurons that showed zero miniature events (spontaneous) even during the application of hypertonic sucrose solution were excluded from our analysis.

2.4. Immunocytochemistry

At DIV12-15 (unless otherwise noted), coverslips with cultured neurons were washed with phosphate buffer saline (PBS) to remove any debris or dead cells and fixed in 4% w/v paraformaldehyde in PBS, pH 7.4 for 10 min at RT. Neurons were washed thrice with PBS for 10 min each. Following permeabilization with PBS with 0.1% Tween (PBST) for 10 min and blocking with 5% v/v normal donkey serum (NDS) in PBST for 1 hr at RT, cells were incubated overnight at 4 ^{0}C with one of the following primary antibody dilutions: (i) mouse anti-VGAT (1:1000; Synaptic Systems, Germany), (ii) chicken anti-microtubule-associated protein 2 (MAP2) (1:2000; Millipore), (iii) guinea pig anti-VGLUT1 (1:4000; Synaptic Systems) and (iv) guinea pig anti-VGLUT2 (1:1000; Synaptic Systems). Coverslips were then washed three times with PBST for 15 min each. Secondary Alexa-Fluor (488, 555 or 647; 1:500; Jackson, West Groove, PA) labeled antibodies were then used for 1 hr at room temperature. As a last step, coverslips were washed twice with PBST and twice with PBS for 15 min each and then mounted on glass slides with Mowiol 40-88 (Sigma-Aldrich).

2.5. Quantification of neuronal morphology

Neuronal morphology was quantified using 16-bit images acquired from an Olympus IX81 inverted epifluorescence microscope at 20x optical magnification (numerical aperture NA = 0.75) with a CCD camera (Princeton MicroMax; Roper Scientific, Trenton, NJ) and MetaMorph software (Molecular Devices). To control for systematic errors and increase statistical power, at least three independent cultures were imaged and analyzed for each experiment. During data acquisition, the investigator was blinded to experimental groups, coverslips were always randomized to drug treatments and images were acquired using equal exposure times.

Soma size and dendritic length were quantified using MAP2 staining. For cell soma size estimation, the cross-sectional area across the MAP2-positive cell body was measured and for total dendrite length, quantification of all MAP2-positive processes with NeuronJ plugin (Meijering et al., 2004) was used. The total number of GABAergic synapses was estimated by manually counting the number of vesicular GABA transporter (VGAT) fluorescent puncta and for

glutamatergic synapses the number of vesicular glutamate transporter type 1, (VGLUT1; for cortex) or 2, (VGLUT2; thalamus) fluorescent puncta. After background subtraction with a rolling ball of a radius of 30 pixels and threshold adjustment, images were converted to binary using ImageJ plugin. Similarly to RRP, in heterotypic pairs the total number of VGAT puncta represented the synapses of the striatal partner, while in homotypic striatal pairs the total number of VGAT puncta was divided by half, assuming an equal number of synapses between the two striatal cells. Raw values were further analyzed in Prism (GraphPad, La Jolla, CA).

2.6. Statistical Analysis

To minimize culture-to-culture variability, data from at least three independent cultures were collected and an approximately equal number of neurons per experimental group was recorded on a given day. Prior to experimental design, sample size estimation was conducted for a statistical power of 0.8. Data are presented as mean ± SEM. The D'Agostino-Pearson test was run for the different variables to test for the normality of the data. In case of normally distributed data, statistical significance was assessed using Student's t test for comparison of two independent groups and one-way ANOVA using Tukey HSD post-hoc test for three or more groups. When data were not normally distributed, Mann-Whitney U test and Kruskal-Wallis test (KW test) coupled with Dunn's post hoc test, for comparison of two or more than two groups respectively, were performed. Statistical analysis was performed in GraphPad Prism v.7 software. * refers to $p \leq 0.05$, ** $p \leq 0.01$, *** $p \leq 0.001$ and **** $p \leq 0.001$.

3. Results

Here, I present the most significant and novel findings of my research. Further details can be found in Paraskevopoulou et al. 2019, Journal of Neuroscience (attached manuscript).

In the following sections I will present the analysis of the total autaptic and heterosynaptic responses. Responses were analyzed as a sum: i) since sucrose application in homotypic pairs (i.e. GABA-GABA pairs) affects both types of synapses (Stevens 1996) and it does not allow to distinguish later for autaptic and heterosynaptic responses, ii) as it allows for the direct comparison between functional and morphological changes, given that our Immunostainings prevent the distinguish between autapses and heterosynapses and iii) to allow for direct comparison between the findings of our study and that of Chang et al. (2014).

3.1 Glutamatergic input from cortex and thalamus potentiates striatal GABAergic neurons' synaptic transmission

In a previous study of our lab, Chang et al., (2014) found that glutamatergic input caused hippocampal GABAergic interneuron to modify its output, increasing the number of synapses and the readily releasable vesicles and decreasing the synaptic release efficiency. In contrast glutamatergic neurons did not change their response in the presence of GABAergic neurons. These provide the necessary basis for the current project. Here, using the same two-neuron microcircuit culture, we examined whether a similar glutamatergic-induced modulation is also present at striatal GABAergic microcircuits. For this purpose, we compared GABAergic release characteristics between cortico-striatal (CS; Glu-GABA) or thalamo-striatal (TS; Glu-GABA) pairs and striatal-striatal GABAergic (control; SS) pairs (Figure 3A-C). To confirm that all changes observed in striatal output are only induced by glutamatergic input and not by any other partner, we also used striatal autaptic neurons as a second control group and compared their electrophysiological properties to striatal homotypic pairs. Noting that in autaptic neurons the synaptic input of a neuron onto itself equals the synaptic output of this neuron.

Using paired whole cell patch-clamp recordings in a voltage clamp configuration, we measured a number of different physiological parameters. Striatal neurons paired with either cortical or thalamic glutamatergic partner revealed an almost two-fold increase in the total (sum of autaptic and heterosynaptic responses; see Materials and Methods) evoked IPSC amplitude (CS: -21.14±3.12 nA, n=29, p=0.006; TS: -19.13±3.29 nA, n=25, p=0.026, KW test) and total RRP charge (CS: -6.30±0.62 nC, n=27, p=0.002; TS: -7.61±0.91 nC, n=24, p=0.001, KW test) (Figure 3D-H) compared to striatal control pairs (SS IPSC: -10.51±1.23 nA, n=60 and RRP: -3.77±0.30 nC, n=54). In contrast to hippocampal findings, no differences were observed in Pvr or PPR measurements (SS: 13.66±1.24%, n=48; CS: 11.64±1.79%, n=27, p=0.625; TS: 14.07±1.76%, n=24, p>0.999, KW test) (Figure 3I-J), indicating that the efficiency of release remained unaffected.

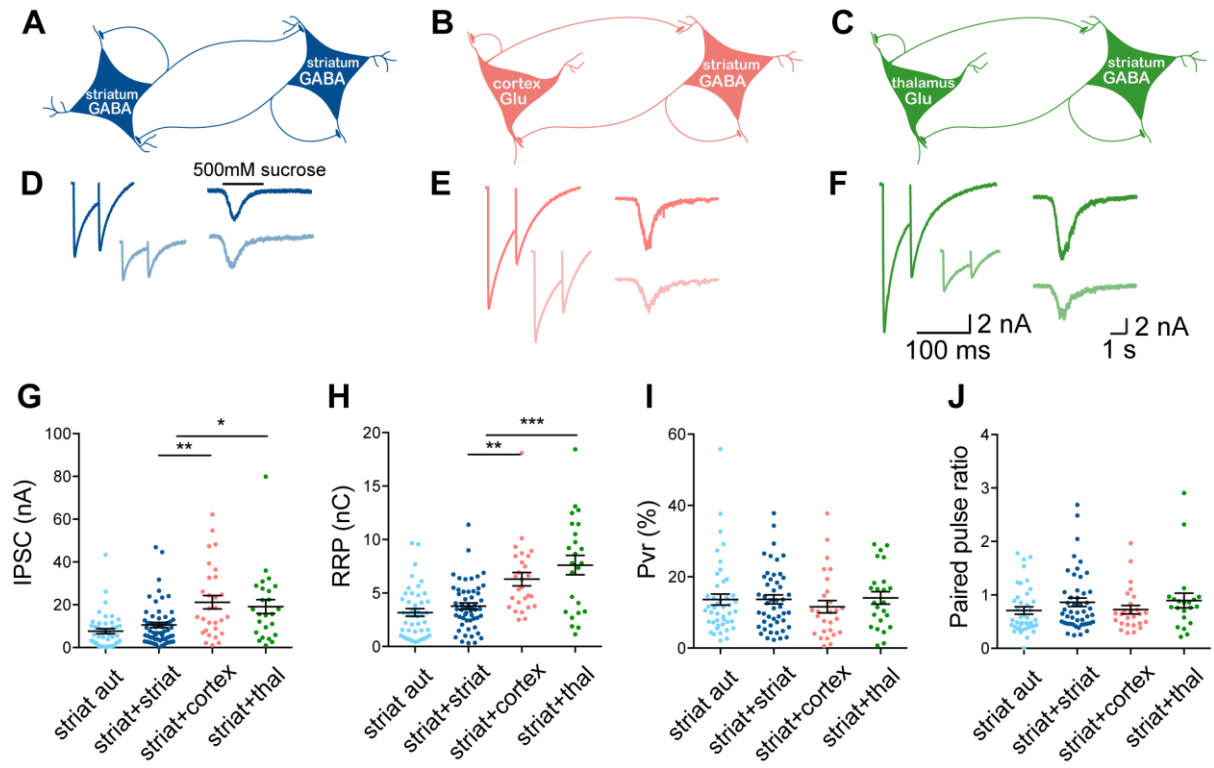

Figure 3. Striatal GABAergic output is potentiated by glutamatergic input. (A-C) Schematic diagram illustrating autaptic and heterosynaptic connections in striatal (GABAergic only; dark blue), cortico-striatal (glu-GABA; pink) and thalamo-striatal (glu-GABA; green) pairs. (D-J) Functional analysis of striatal autapses (light blue traces and dots), striatal pairs (blue traces and dark blue dots), cortico-striatal pairs (pink traces and dots) and thalamo-striatal pairs (green traces and dots). (D-F) Representative traces of GABAergic response to paired pulse stimulation with 50 ms inter-stimulus interval and to a 5 second pulse of 500 mM hypertonic sucrose solution (dark; autaptic, light; heterosynaptic). (G-J) Scatter plots showing total evoked IPSC amplitudes (G), RRP size (H), Pvr% (I) and PPR (J). Mean ± SEM. * refers to $p \leq 0.05$, ** $p \leq 0.01$ and *** $p \leq 0.001$.

We next tested whether spontaneous release of striatal neurons was also affected by the presence of a glutamatergic partner. Pairing of striatal neurons with either cortical or thalamic glutamatergic neurons resulted in an increase of mIPSC amplitude (SS: -44.31±3.04 pA, n=42; CS: -74.24±7.07 pA, n=38, p=0.002; TS: -79.17±8.16 pA, n=32, p=0.001, KW test) (Figure 4A-D), and mIPSC charge (SS: -838.10±68.96 fC, n=42; CS: -1379±129.2 fC, n=38, p=0.004; TS: -1454±172.5 fC, n=32, p=0.01, KW test), compared to control striatal pairs, demonstrating that glutamatergic input strengthens striatal inhibition to itself and to the glutamatergic partner neuron (Figure 4E). Conversely, the frequencies of inhibitory miniature events were comparable among groups (SS: 2.15±0.26 Hz, n=42; CS: 1.70±0.35 Hz, n=41, p=0.121; TS: 2.54±0.47 Hz, n=36, p>0.999, KW test), suggesting no change in presynaptic release (Figure 4F). To further investigate whether the increased inhibitory transmission we observed in heterotypic pairs, is due to the higher number of fusion competent synaptic vesicles (RRP vesicles), we calculated RRP vesicles by dividing the total output RRP charge by the average charge of the miniature events from the same

neuron. Interestingly, we found that only in the case of cortical partner, the number of vesicles released from the striatal neuron was increased (SS: 4445±362, n=35; CS: 8498±1700, n=16, p=0.04; TS: 5197±990, n=14, p>0.999, KW test) (Figure 4G). This suggests a differential role between cortical and thalamic input; in which cortico-striatal projections promote inhibitory transmission by affecting striatal postsynaptic sensitivity to GABA release and the number of RRP vesicles, whereas thalamo-striatal projections increase striatal GABAergic output by only causing a postsynaptic change, as supported by the alteration in mIPSC size.

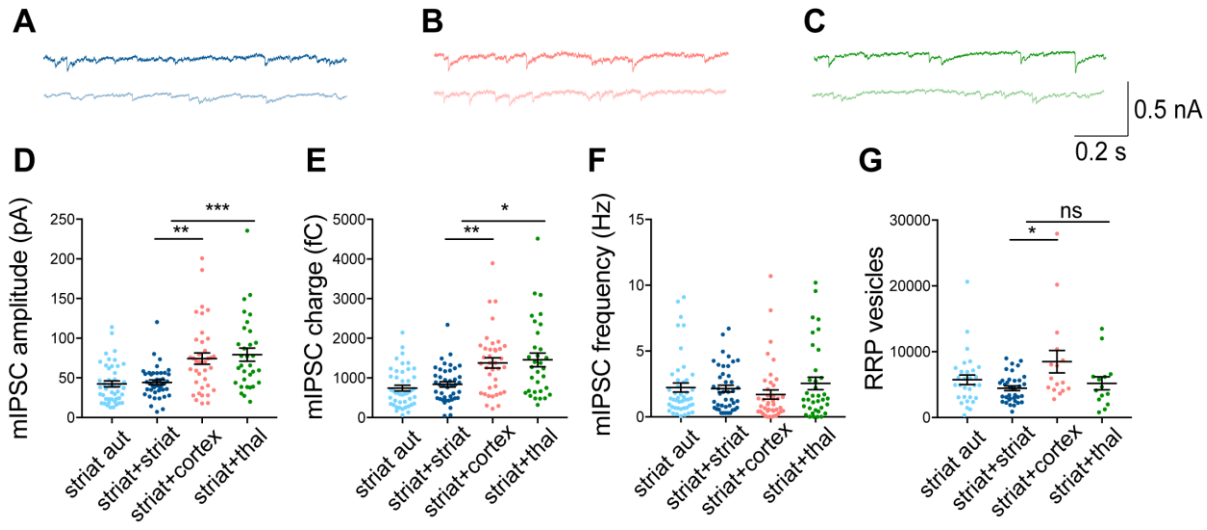

Figure 4. Distinct cortical- and thalamic-induced mechanisms for the modulation of striatal output. (A-C) Representative traces showing miniature postsynaptic current activity of striatal neurons in striatal pairs (blue), cortico-striatal (pink) and thalamo-striatal (glu-GABA; green) pairs (dark; autaptic, light; heterosynaptic). (D-G) Scatter plots showing mean mIPSC amplitudes (D), charge (E), frequency (F), and RRP vesicles number (G). Mean ± SEM. ns refers to not significant, * $p \leq 0.05$, ** $p \leq 0.01$ and *** $p \leq 0.001$.

3.2 Cortical input promotes synapse formation in striatal GABAergic neurons

The cortical-induced increase in the number of RRP vesicles measured with the electrophysiological recordings could either reflect a higher number of vesicles per synapse or the formation of more synapses. To distinguish between these two possibilities, we analyzed the morphology of striatal neurons among groups and quantified the number of VGAT puncta; a marker of presynaptic inhibitory synapses. Our findings showed that although the number of inhibitory synapses in cortico-striatal pairs was increased, there was no change in the number of GABAergic synapses in thalamo-striatal pairs, compared to control striatal pairs or autapses (SS: 174.8±17.48, n=23; CS: 326.3±41.52, n=21, p=0.009; TS: 175.4±17.72, n=26, p>0.999, KW test) (Figure 5A-B). This result was consistent with our electrophysiological findings that revealed a higher number of RRP vesicles only in presence of cortical partner and verified our assumption

that this was caused by an increase in the number of inhibitory synaptic contacts. Furthermore, when we assessed the number of glutamatergic synapses by counting VGLUT1 for cortical and VGLUT2 for thalamic synapses, we found a higher number of glutamatergic synapses of cortical neurons over striatal cells (CS: 312.2±38.7, n=23; TS: 118.2±15.5, n=25, p<0.0001, Mann-Whitney test) (Figure 5C). Therefore, our results suggest that the difference in striatal output modulation by cortical and thalamic partners is due to the magnitude of glutamatergic input. This result was further supported by our electrophysiological measurements in heterotypic pairs, in which cortical evoked release was double compared to thalamic (EPSC CS: -9.78±1.53 nA, n=30; TS: -4.72±0.95 nA, n=25, p=0.006, Mann-Whitney test).

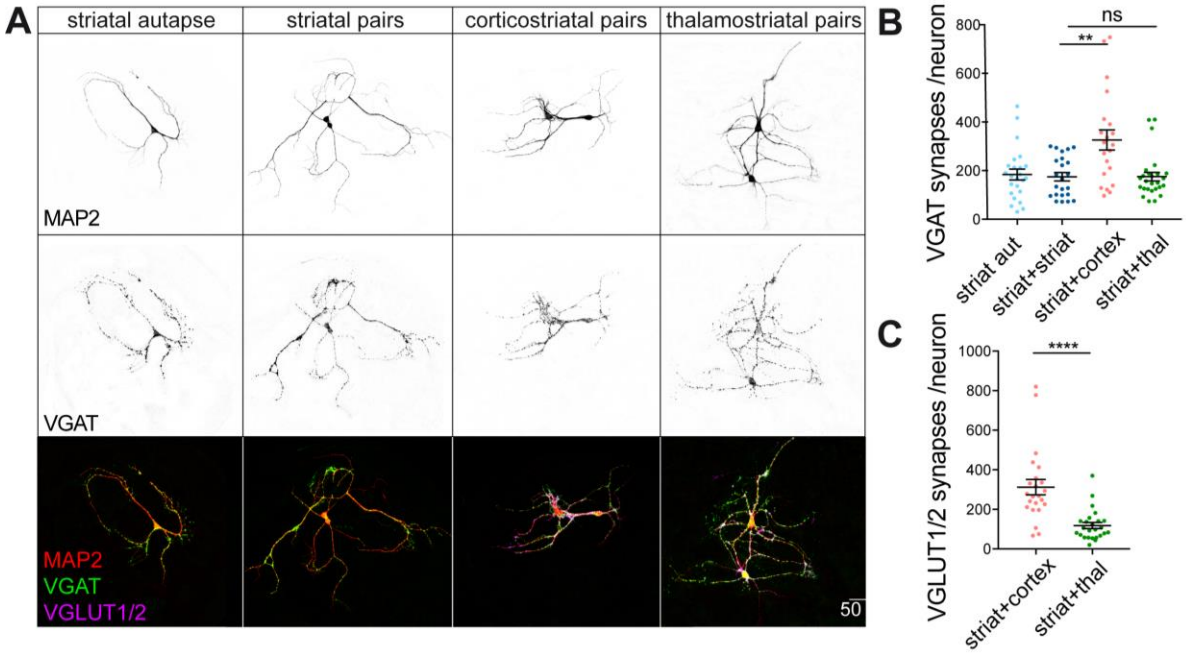

Figure 5. Cortical input increases the number of GABAergic synapses in striatal neurons. (A-B) Morphological analysis of striatal autapses (light blue dots), striatal pairs (dark blue dots), cortico-striatal pairs (pink dots) and thalamo-striatal pairs (green dots). (A) Representative images of neuronal morphology showing immunoreactivity for MAP2, VGAT and VGLUT1 or VGLUT2. (B-C) Scatter plots showing number of VGAT synapses per neuron (B) and VGLUT1 (in cortico-striatal pairs) or VGLUT2 (in thalamo-striatal pairs) synapses per neuron (C). Mean ± SEM. ns refers to not significant, ** $p \leq 0.01$ and **** $p \leq 0.0001$.

3.3 Neuronal activity and glutamatergic firing is required for inhibitory synapse formation in cortico-striatal pairs

To better understand the putative mechanisms in regulating inhibitory synapse formation, we focused on the factors that could be responsible for the changes induced in the striatal neurons in the case of the cortico-striatal pairs. We have shown that cortical input potentiated inhibitory transmission of striatal neurons *in vitro*. Given that neuronal activity has been shown to shape the

striatal output (Stern et al., 1997) and that the only source of excitation onto striatal neurons comes from the glutamatergic innervation, we chronically blocked action potential firing with TTX (0.5 µM) or glutamate receptor signaling with a cocktail of NBQX (2 µM) /APV (100 µM) antagonists. Drugs were always applied to the culture media at DIV 3, 7, 11 and neurons were recorded between DIV 12-15.

Upon treatment with TTX, IPSC amplitude in cortico-striatal pairs was reduced by 59% (CS: -17.93±1.87 nA, n=37; CS+TTX: -7.34±1.25 nA, n=21, p=0.005, KW test) and RRP by 42% (CS: -6.75±0.67 nC, n=37; CS+TTX: -3.88±0.66 nC, n=20, p=0.05, KW test), compared to untreated cortico-striatal pairs (Figure 6A-B). Likewise, blockade of glutamate receptors in cortico-striatal pairs caused a 58% reduction in IPSC (CS+NBQX/APV: -7.50±0.89 nA, n=18, p=0.041, KW test) and 50% decrease in RRP (CS+NBQX/APV: -3.39±0.58 nC, n=19, p=0.008, KW test), compared to untreated cortico-striatal pairs (Figure 6A-B). In regards to striatal spontaneous release and the number of RRP vesicles released, we observed that in heterotypic pairs, upon treatment with either antagonist (TTX or NBQX/APV), both physiological parameters were reduced back to the levels of control striatal pairs (mIPSC amplitude SS: -55.15±4.28, n=47; CS: -77.56±4.51 pA, n=69; CS+TTX: -50.61±4.23 pA, n=34, p=0.001; CS+NBQX/APV: -54.62±5.15 pA, n=29, p=0.028, KW test and RRP vesicles SS: 2740±450.7, n=34; CS: 5988±716.1, n=35; CS+TTX: 2963±451.9, n=19, p=0.187; CS+NBQX/APV: 2837±388.6, n=19, p=0.144, KW test) (Figure 6C,D). Striatal homotypic pairs did not show any changes in their synaptic output upon application of any drug, indicating that action potential generation and activation of glutamate signaling on them is cortical input-specific (Figure 6A-D). In all experimental conditions, Pvr or PPR remained unchanged. Together, these findings illustrate the significance of cortical activity in the modulation of striatal synaptic output.

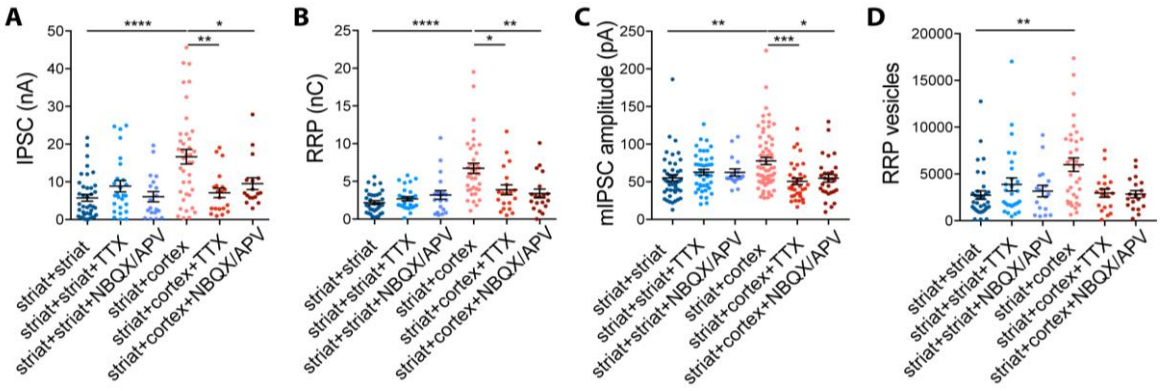

Figure 6. Activity modulates GABAergic synapse output in cortico-striatal pairs. (A-F) Functional analysis of striatal pairs (blue color scale dots), cortico-striatal pairs (red color scale dots). Scatter plots showing total evoked IPSC amplitudes (A), RRP size (B), mIPSC amplitudes (C) and RRP vesicles number (D). Mean ± SEM. * indicates $p \leq 0.05$, ** $p \leq 0.01$, *** $p \leq 0.001$ and **** $p \leq 0.0001$.

3.4 Activity-dependent BDNF release promotes GABAergic synapse formation and function in cortico-striatal pairs

BDNF is an activity-dependent gene, crucial for the regulation of GABAergic synapse formation and function (Park and Poo, 2013). Although *Bdnf* is not expressed in the striatum, BDNF protein is already present in this region at E16.5. Thus, recent studies argue that cortex and thalamus are the main sources of BDNF release onto the striatal neurons (Baydyuk and Xu, 2014). To assess if BDNF release by cortical neurons is the signal linking the activity to the regulation of inhibitory synapse formation, we disrupted the BDNF-TrkB receptor signaling pathway with the use of Trk inhibitor K252a (200 µM; at DIV3, 7, 11).

Incubation of cortico-striatal pairs with K252a prevented the cortical-induced increase in both physiological and morphological phenotypes (Figure 7). We found that chronic treatment with K252a inhibitor reduced evoked IPSC amplitude and RRP size in cortico-striatal pairs, compared to untreated heterotypic pairs (IPSC SS: -5.21±0.89 nA, n=44; CS: -10.38±1.23 nA, n=54, p=0.007; CS+K252a: -7.73±1.47 nA, n=32, p=0.042, KW test and RRP SS: -2.29±0.26 nC, n=37; CS: -4.58±0.37 nC, n=49, p<0.0001; CS+K252a: -2.74±0.38 nC, n=31, p=0.003, KW test) (Figure 7A,B). Similar results were observed for mIPSC amplitude (SS: -42.96±2.58 pA, n=40; CS: -66.59±4.64 pA, n=63, p=0.013; CS+K252a: -46.82±3.55 pA, n=58, p=0.009, KW test) and the number of RRP vesicles (SS: 3364±452.8, n=33; CS: 5846±605.6, n=49, p=0.013; CS+K252a: 4136±724.9, n=30, p=0.067, KW test) (Figure 7C,D). Importantly, cortical-effect specificity to BDNF-TrkB signaling was verified by the absence of K252a effect in striatal pairs. The same findings were also confirmed by morphological analysis of synapses in cortico-striatal pairs. In particular, it was revealed that blockade of TrkB receptors negated the formation of functional inhibitory synapses (CS: 498.5±63.2, n=32; CS+K252a: 269.3±30.89, n=29, p=0.048, KW test), as well as reduced the total number of glutamatergic synapses formed by the cortical neurons (CS: 570.6±52.46, n=35; CS+K252a: 377.5±45.63, n=27, p=0.03, KW test) (Figure 7E-G).

As an additional control experiment, to further investigate the BDNF-mediated GABAergic synapse formation, we blocked BDNF function by treating cortico-striatal pairs with an anti-BDNF neutralizing antibody (10 ng/ml; at DIV3, 7, 11). The comparison between treated and untreated heterotypic pairs revealed that BDNF neutralization also prevented the formation of inhibitory synapses (CS: 498.5±63.2, n=32; CS+anti-BDNF: 197.7±22.99, n=33, p<0.0001, KW test) and reduced the total number of glutamatergic synapses formed by the cortical neurons (CS: 570.6±52.46, n=35; CS+anti-BDNF: 314.8±29.01, n=33, p=0.001, KW test) (Figure 7E-G).

Overall, these observations emphasized the impact of activity-dependent BDNF release onto striatal synapses formation and function.

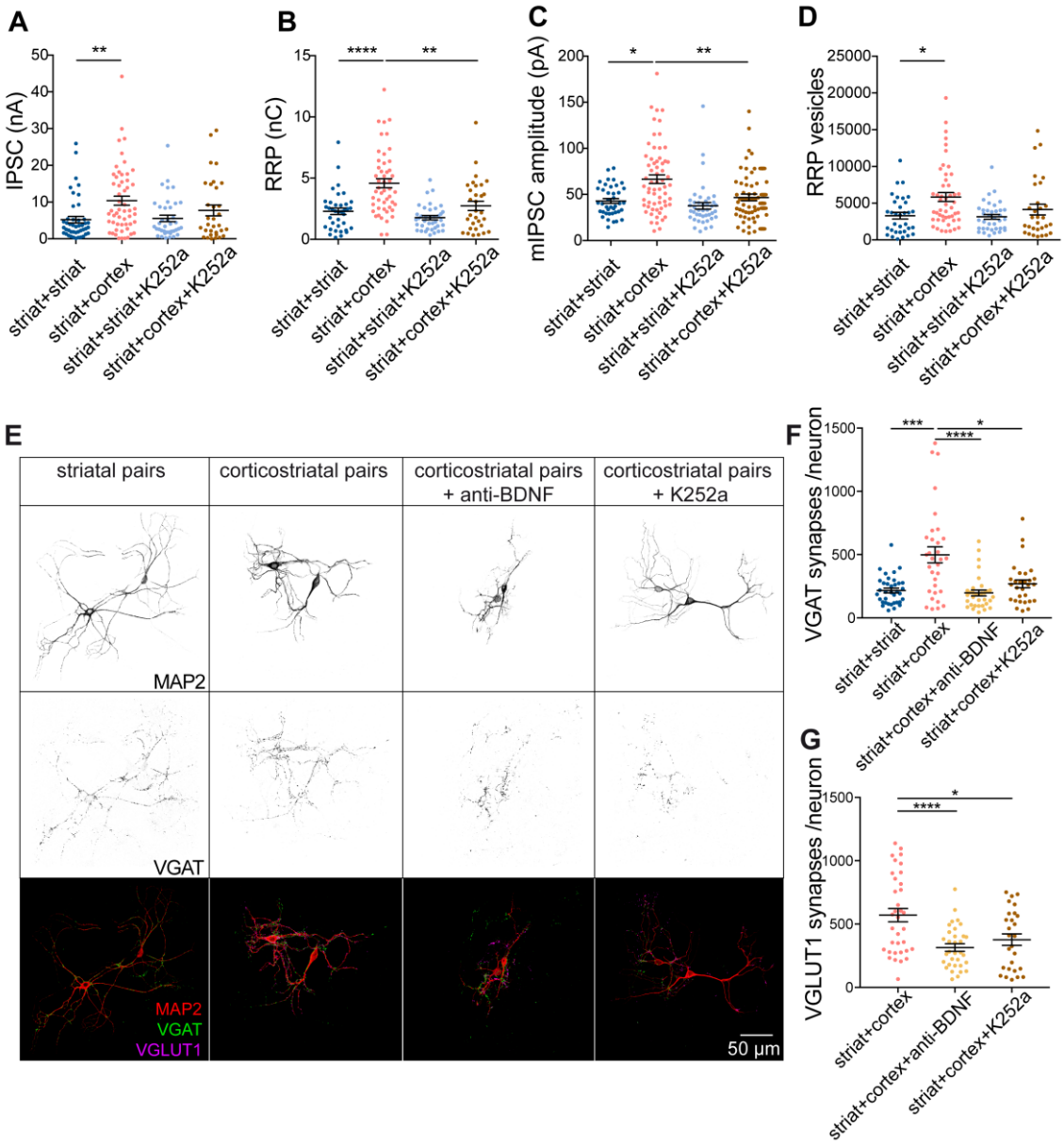

Figure 7. BDNF release modulates GABAergic synapse output and synapse number in cortico-striatal pairs. (A-D) Functional analysis of striatal pairs (untreated; dark blue, Trk-antagonist treated; purple), cortico-striatal pairs (untreated; pink, Trk-antagonist treated; brown). Scatter plots showing mean evoked IPSC amplitudes (A), RRP size (B), mIPSC amplitudes (C) and RRP vesicles number (D). (E) Representative images of neuronal morphology showing immunoreactivity for MAP2, VGAT and VGLUT1. (F-G) Scatter plots showing the number of VGAT synapses per neuron (F), the number of VGLUT1 synapses per neuron (G). Mean ± SEM. * indicates $p \leq 0.05$, ** $p \leq 0.01$, *** $p \leq 0.001$ and **** $p \leq 0.0001$.

4. Discussion

How glutamatergic input shapes striatal output remains an open question. Although, previous studies have focused on quantifying glutamatergic-induced morphological changes in striatum

(Segal et al., 2003; Kaufman et al., 2012), we still know little about glutamatergic input effect on striatal excitability. This is hindered by the technical challenges that emerge due to the long distances of inter-regional connections and the divergent connections of striatal neurons with their targeted areas. Our research emphasizes the power of an *in vitro* approach to study the functional properties of neuronal connections that are formed between two distant brain regions *in vivo*. Here, we used a two-neuron *in vitro* dissociated culture system to distinguish the functional properties of cortico-striatal and thalamo-striatal connections and separately assess their impact on striatal neuron physiology and morphology. In fact, in our model, the target neurons are the same with the input neurons because of the connectivity pattern of the system. Although, this may seem a weakness of the system, we argue that in the present study these interactions are one of its main advantages. In our approach, neurons form tiny circuits and at the same time the input and the output of each neuron are not distributed to a heterogeneous population of cells. These allow us to study their responses more accurately. Furthermore, using pharmacological approaches we isolated the contribution of individual glutamatergic input components and gained insight into the underlying mechanisms that drive glutamatergic-induced changes in striatal neurons. Our findings indicated that glutamatergic input from cortex and thalamus modulates striatal GABAergic neuron synaptic transmission by potentiating their output. Striatal output potentiation was mediated by two separate mechanisms. The first one involved an increase in the strength of striatal inhibition and was observed in both cortico-striatal and thalamo-striatal connections, while the second mechanism was unique for cortico-striatal connections and involved an increased inhibitory synapse formation. Cortical-induced potentiation of striatal GABAergic neurons required glutamatergic firing, postsynaptic glutamate receptor activation and activity dependent BDNF release. To the best of our knowledge, this is the first study that quantifies the functional synaptic output from striatal GABAergic neurons innervated by a glutamatergic partner. Together, our findings indicate that both neuronal activity and BDNF release from cortical neurons work in concert to regulate multiple aspects of striatal GABAergic function.

4.1. Cortical and thalamic glutamatergic neurons potentiate striatal GABAergic output in distinct ways

Glutamatergic inputs from cortical and thalamic regions are known to project to striatum, inducing MSNs firing. Studies in brain slices showed that despite their common glutamatergic phenotype, cortical and thalamic synapses differ in their properties and the way they determine striatal output (Ding et al., 2008; Doig et al., 2010). At presynaptic terminals, cortico-striatal synapses display

paired-pulse facilitation due to a low quantal release probability, whereas thalamo-striatal synapses reveal synaptic depression and high release efficiency. Although such studies explored the distinctive properties of cortico-striatal and thalamo-striatal synapses, a clear explanation of how the different inputs influence MSN excitability is still missing. To fill this knowledge gap, here we used membrane dye labeling of neurons from the specific brain regions and two-neuron microcircuits, to directly assess and quantify the interaction between excitatory projections and the principal neurons of striatum. Our results indicated for the first time that both cortical and thalamic projections doubled the evoked inhibitory postsynaptic response and RRP size of their striatal counterparts (Figure 3G,H). For both partners, this potentiation was attributed to an increased strength of individual striatal synapses (Figure 4D). In addition to that, cortico-striatal projections caused an increase in the number of GABAergic synapses (Figure 5B). This differential effect of cortical versus thalamic innervation most likely originates from the higher synaptic strength that cortical projections revealed compared to thalamic ones. *In vivo* studies have indeed shown that synapses from cortex are denser and control the activity patterns of MSNs though the transition from a hyperpolarized (non active) to depolarized state (Wilson, 1993; Ingham et al., 1998), whereas thalamic synapses are less profuse and give rise to a rather sparse population of terminals (Bevan et al., 1995; Smith et al., 2004). In agreement with these observations, we revealed that the number of excitatory synapses in cortico-striatal pairs was higher compared to thalamo-striatal pairs (Figure 5C). This resulted in a stronger modulation of striatal cells by cortical neurons, and the formation of more functional inhibitory synapses (Figure 5B). At the network level, striatal neurons communicate with each other via local axon collaterals, forming recurrent inhibitory synaptic contacts (Taverna et al., 2008). It is likely that the distinct functional properties of cortico-striatal and thalamo-striatal synapses differentially affect MSNs communication and thus serve as modulators of different brain functions.

4.2. Cortical-induced potentiation of striatal GABAergic output requires neuronal activity and activity-dependent BDNF release

Previous *in vitro* studies in hippocampus have revealed that GABAergic synapse formation is activity-mediated (Marty et al., 1996; Hartman et al., 2006; Chang et al., 2014). Additionally, Segal et al. (2003) showed that in cortico-striatal embryonic co-cultures the presence of TTX in growth media prevented the increase in the density of striatal spines caused by cortical input. To determine whether the level of glutamatergic neuron activity modulates the striatal GABAergic output, we conducted electrophysiological recordings in striatal and cortico-striatal pairs. Our

findings indicated that blockade of action potential generation with TTX reduced both striatal inhibitory response and RRP size, compared to untreated cortico-striatal pairs (Figure 6A,B).

To investigate the signals that trigger the change in striatal GABAergic synaptogenesis and identify the pathways involved, we followed a two-fold approach. First, we chronically treated cortico-striatal pairs with glutamate receptors antagonists (NBQX and APV). The comparison between treated and untreated heterotypic pairs showed a significant reduction of striatal inhibitory transmission in the former, suggesting that glutamate signaling is required for the modulation of striatal neurons' synapse formation and maintenance by cortical input (Figure 6A-D). Second, we explored the involvement of BDNF-TrkB pathway in cortical-induced striatal synapse formation and function. Traditionally, it has been suggested that neurotrophins, and particularly BDNF secretion, is the signal responsible for linking activity to the regulation of glutamatergic-induced synapse formation in GABAergic cells (Huang et al., 1999; Hong et al., 2008; Park and Poo, 2013). Multiple lines of evidence show that deletion of BDNF during development leads to decreased survival of MSNs and reduced dendritic arborization in the surviving MSNs (Baquet, 2004; Rauskolb et al., 2010; Baydyuk et al., 2011; Cazorla et al., 2014). Likewise, *in vitro* application of BDNF to striatal culture significantly enhances cellular growth and dendritic arborization (Rauskolb et al., 2010; Penrod et al., 2015; Paraskevopoulou et al., 2019). However, despite the marked progress that has been made in understanding the effect of BDNF in striatal neuron morphology and survival, little is known about the impact of BDNF on striatal physiology. Given that cortical input is the major source of BDNF release onto the striatal neurons (Baydyuk and Xu, 2014), we assessed the effect of BDNF on striatal output in paired neurons. Our experiment showed that blockage of BDNF-TrkB pathway by Trk antagonist K252a prevented cortical-induced changes in striatal neurons' physiology and morphology (Figure 7). To further support the regulatory role of BDNF signaling in striatal neurons' synapse formation, we blocked BDNF function using an anti-BDNF neutralizing antibody and found that increase in the number of inhibitory synapses by cortical input was mediated by BDNF release (Figure 7E,G). Together, our results illustrate that BDNF-TrkB signaling pathway is essential for linking activity to GABAergic synapse formation.

5. Conclusions

Understanding how cortical and thalamic inputs refine striatal output represents an important next step towards dissecting basal ganglia activity in both physiological and pathological conditions. From this point of view, using a two-neuron microcircuit culture model, our study provides new

insights into the properties of connections made between two distant brain regions and explains the contribution of individual glutamatergic input components into the underlying mechanisms that drive glutamatergic-induced changes in striatal neurons. Glutamatergic innervation enhanced striatal GABAergic inhibition, by increasing evoked response and vesicle pool size without affecting the release probability of individual synapses. In particular, a differential effect of thalamic and cortical innervation onto striatal GABAergic neurons output was revealed, where GABAergic synapse formation was promoted only from cortical partner. Furthermore, we showed that neuronal activity and activity-dependent BDNF release were responsible for the increased striatal inhibition in cortico-striatal connections, pointing their synergetic role in synapse formation. Nowadays that an increasing number of studies suggest that basal ganglia circuit dysfunction is a causative factor for the development of movement abnormalities in neurological diseases, including Huntington's disease (Cepeda et al., 2003) and Tourette and Parkinson's syndromes (Henderson et al., 2000; Kalanithi et al., 2005; Smith et al., 2009; Pappas et al., 2014), our two-neuron microcircuit model could be a valuable tool for studying synaptic properties of such disease models in cellular context.

6. Outlook

In this study, we have identified fundamental mechanisms of the striatal GABAergic neuron's output modulation by glutamatergic input under basal conditions. In our ongoing experiments, we intend to extend these findings to pathological conditions and investigate the underlying transcriptional changes occurring in striatal neurons upon glutamatergic innervation. Neuropsychiatric disorders such as autism spectrum disorders (ASD), including Rett syndrome (Shepherd and Katz, 2011) and neurological disorders such as Huntington's disease (Cepeda et al., 2003; Deng et al., 2014) are associated with cortico-striatal and thalamo-striatal circuits misbalance. Particularly, Rett syndrome is a neurodevelopmental disorder (6-18 months of age) caused by mutations in the methyl-CpG-binding protein 2 (MECP2) gene and, among other symptoms, affected individuals show motor deficits (Hagberg et al., 1983). Mecp2-based mouse models of Rett syndrome reveal reduced levels of BDNF expression in the cortex, impaired synaptic output and synapse formation in cortical glutamatergic neurons, and decreased GABA synthesis in striatal GABAergic neurons (Chang et al., 2006; Chao et al., 2007, 2010). On the other hand, Huntington's disease (HD) is a progressive neurodegenerative disorder characterized by motor, cognitive and psychiatric symptomatology (Vonsattel and DiFiglia, 1998). The disease is caused by a mutation in Huntingtin (*HTT*) gene resulting in a neuronal degeneration mainly in

striatum and cortex (Heinsen et al., 1994). The two long-standing hypotheses for the development of the symptoms and the synaptic dysfunction in cortico-striatal pathway are the dysregulation of glutamate release and/or the deprivation of BDNF (Zuccato et al., 2001; Cepeda et al., 2007). On the basis of these findings that motor deficits, caused by MeCP2 deficiency or *HTT* mutation, are associated with a cortico-striatal dysfunction, our two-neuron microcircuit cell culture system is at present the most efficient method to study the interaction of cortical glutamatergic and striatal GABAergic neurons in RTT or HD and identify the pathogenic mechanisms of these diseases (Paraskevopoulou unpublished data).

Another important set of experiments for the comprehensive understanding of synaptic dysfunction in disease involves the advanced knowledge of gene expression of individual cells. In basal ganglia circuits, the pattern of connectivity between neurons determines the degree of activation of striatal projection neurons and, as such, shapes their transcriptional profile that in turn is bound to change their synaptic output. Identifying which genes are affected upon glutamatergic innervation and how they control the functional properties of neurons (i.e. synapse number, release probability) will help us understand the causal mechanistic pathways and identify potential treatments for brain-related diseases. During my PhD, I identified a number of these genes for HD using single-cell RNA-Seq (Patch-seq; Cadwell et al., 2016; Paraskevopoulou et al., *In preparation*). Additionally, using the novel Drop-seq technology I examined how MeCP2 deficiency affects the transcriptional profile of excitatory and inhibitory neurons and how these changes in gene expression are dependent on the BDNF-TrkB pathway (Paraskevopoulou et al., *In preparation*). Overall, our two-neurons system provides a highly controlled environment, in which we elicit cortico-striatal neurons interaction, and an ability to assess the details of this process - from physiological to transcriptional changes- at a single-cell level.

7. References

Albin RL, Young AB, Penney JB (1989) The functional anatomy of basal ganglia disorder. Trends Neurosci 12:366–375.

Baquet ZC (2004) Early Striatal Dendrite Deficits followed by Neuron Loss with Advanced Age in the Absence of Anterograde Cortical Brain-Derived Neurotrophic Factor. J Neurosci 24:4250–4258.

Baydyuk M, Russell T, Liao G-Y, Zang K, An JJ, Reichardt LF, Xu B (2011) TrkB receptor controls striatal formation by regulating the number of newborn striatal neurons. Proc Natl Acad Sci 108:1669–1674.

Baydyuk M, Xu B (2014) BDNF signaling and survival of striatal neurons. Front Cell Neurosci 8:254.

Bekkers JM, Stevens CF (1991) Excitatory and inhibitory autaptic currents in isolated hippocampal neurons maintained in cell culture. Proc Natl Acad Sci 88:7834–7838.

Bevan MD, Francis C, Bolam JP (1995) The glutamate enriched cortical and thalamic input to neurons in the subthalamic nucleus of the rat: Convergence with GABA positive terminals. J Comp Neurol 361:491–511.

Brünig I, Penschuck S, Berninger B, Benson J, Fritschy J-M (2001) BDNF reduces miniature inhibitory postsynaptic currents by rapid downregulation of GABAA receptor surface expression. Euro 13:1320–1328.

Cadwell CR, Palasantza A, Jiang X, Berens P, Deng Q, Yilmaz M, Reimer J, Shen S, Bethge M, Tolias KF, Sandberg R, Tolias AS, Institutet K (2016) Electrophysiological, transcriptomic and morphologic profiling of

single neurons using Patch-seq. Nat Biotechnol 34:199–203.
Cazorla M, de Carvalho FD, Chohan MO, Shegda M, Chuhma N, Rayportm S, Ahmari SE, Moore H, Kellendonk C (2014) Dopamine D2 receptors regulate the anatomical balance of basal ganglia circuitry. Neuron 81:153–164.
Cepeda C, Hurst RS, Calvert CR, Hernández-Echeagaray E, Nguyen OK, Jocoy E, Christian LJ, Ariano MA, Levine MS, Herna E, Nguyen OK, Jocoy E, Christian LJ, Ariano MA, Levine MS (2003) Transient and progressive electrophysiological alterations in the corticostriatal pathway in a mouse model of Huntington's disease. J Neurosci 23:961–969.
Cepeda C, Wu N, Andre VM, Cummings DM, Levine MS (2007) The Corticostriatal Pathway in Huntington's Disease. Prog Neurobiol 81:253–271.
Chagnac-Amitai Y, Connors BW (1989) Horizontal Spread of Synchronized Activity in Neocortex and its Control by GABA-Mediated Inhibition. J Neurophysiol 61:747–758.
Chang C, Trimbuch T, Chao H, Jordan J, Herman MA, Rosenmund C (2014) Investigation of Synapse Formation and Function in a Glutamatergic-GABAergic Two-Neuron Microcircuit Chia-Ling. J Neurosci 34:855–868.
Chang Q, Khare G, Dani V, Nelson S, Jaenisch R (2006) The Disease Progression of Mecp2 Mutant Mice Is Affected by the Level of BDNF Expression. Neuron 49:341–348.
Chao H, Chen H, Samaco RC, Xue M, M C, Yoo J, Neul JL, Gong S, Lu H, Heintz N, Ekker M, Rubenstein JLR, Noebels JL, Rosenmund C, Zoghbi HY (2010) GABAergic dysfunction mediates autism-like stereotypies and Rett syndrome phenotypes. Nature 468:263–269.
Chao H, Zoghbi HY, Rosenmund C (2007) MeCP2 Controls Excitatory Synaptic Strength by Regulating Glutamatergic Synapse Number. Neuron 56:58–65.
Chattopadhyaya B, Cristo G Di, Higashiyama H, Knott GW, Kuhlman SJ, Welker E, Huang ZJ (2004) Experience and Activity-Dependent Maturation of Perisomatic GABAergic Innervation in Primary Visual Cortex during a Postnatal Critical Period. J Neurosci n 24:9598–9611.
DeLong MR (1990) Primate models of movement disorders of basal ganglia origin. Trends Neurosci 13:281–285.
Deng Y, Wong T, Wan JY, Reiner A (2014) Differential loss of thalamostriatal and corticostriatal input to striatal projection neuron types prior to overt motor symptoms in the Q140 knock-in mouse model of Huntington's disease. Front Syst Neurosci 8:198.
Ding J, Peterson JD, Surmeier DJ (2008) Corticostriatal and Thalamostriatal Synapses Have Distinctive Properties. J Neurosci 28:6483–6492.
Doig NM, Moss J, Bolam JP (2010) Cortical and Thalamic Innervation of Direct and Indirect Pathway Medium-Sized Spiny Neurons in Mouse Striatum. J Neurosci 30:14610–14618.
Gerfen CR (1984) The neostriata I mosaic: compartmentalization of corticostriatal input and striatonigral output systems. Nature 311:461–464.
Gerfen CR (1992) The neostriatal mosaic: multiple levels of compartmental organization. Trends Neurosci 15:133–139.
Graybiel AM (2000) The basal ganglia. Curr Biol 10:509–511.
Hagberg B, Aicardi J, Dias K, Ramos O (1983) A Progressive Syndrome of Autism, Dementia, Ataxia, and Loss of Purposeful Hand Use in Girls: Rett' s Syndrome : Report of 35 Cases. Ann Neurol 14:471–479.
Hartman KN, Pal SK, Burrone J, Murthy VN (2006) Activity-dependent regulation of inhibitory synaptic transmission in hippocampal neurons. Nat Neurosci 9:642–649.
Heinsen H, Strik M, Bauer M, Luther K, Ulmar G, Gangnus D, Jungkunz G, Eisenmenger W, Götz M (1994) Cortical and striatal neurone number in Huntington ' s disease. Acta Neuropathol 88:320–333.
Henderson JM, Carpenter K, Cartwright H, Halliday GM (2000) Loss of thalamic intralaminar nuclei in progressive supranuclear palsy and Parkinson's disease: clinical and therapeutic implications. Brain 123:1410–1421.
Hong EJ, Mccord AE, Greenberg ME (2008) A biological function for the neuronal activity-dependent component of Bdnf transcription in the development of cortical inhibition. Neuron 60:610–624.
Huang ZJ (2009) Activity-dependent development of inhibitory synapses and innervation pattern : role of GABA signalling and beyond. J Physiol 9:1881–1888.
Huang ZJ, Kirkwood A, Pizzorusso T, Porciatti V, Morales B, Bear MF, Maffei L, Tonegawa S (1999) BDNF regulates the maturation of inhibition and the critical period of plasticity in mouse visual cortex. Cell 98:739–755.
Ingham CA, Hood SH, Taggart P, Arbuthnott GW (1998) Plasticity of synapses in the rat neostriatum after unilateral lesion of the nigrostriatal dopaminergic pathway. J Neurosci 18:4732–4743.
Kalanithi PSA, Zheng W, Kataoka Y, DiFiglia M, Grantz H, Saper CB, Schwartz ML, Leckman JF, Vaccarino FM (2005) Altered parvalbumin-positive neuron distribution in basal ganglia of individuals with Tourette syndrome. Proc Natl Acad Sci 102:13307–13312.
Kaufman AM, Milnerwood AJ, Sepers MD, Coquinco A, She K, Wang L, Lee H, Craig AM, Cynader M, Raymond LA (2012) Opposing Roles of Synaptic and Extrasynaptic NMDA Receptor Signaling in Cocultured Striatal and Cortical Neurons. J Neurosci 32:3992–4003.

Kilman V, Rossum MCW Van, Turrigiano GG (2002) Activity Deprivation Reduces Miniature IPSC Amplitude by Decreasing the Number of Postsynaptic GABAA Receptors Clustered at Neocortical Synapses. J Neurosci 22:1328–1337.

Kreitzer AC, Malenka RC (2008) Striatal plasticity and basal ganglia circuit function. Neuron 60:543–554.

Marty S, Berninger B, Carroll P, Thoenen H (1996) GABAergic Stimulation Regulates the Phenotype of Hippocampal Interneurons through the Regulation of Brain-Derived Neurotrophic Factor. Neuron 16:565–570.

Marty S, Wehrlé R, Sotelo C (2000) Neuronal activity and brain-derived neurotrophic factor regulate the density of inhibitory synapses in organotypic slice cultures of postnatal hippocampus. J Neurosci 20:8087–8095.

Meijering E, Jacob M, Sarria JF, Steiner P, Hirling H, Unser M (2004) Design and Validation of a Tool for Neurite Tracing and Analysis in Fluorescence Microscopy Images. Cytometry 58:167–176.

Nelson SB, Valakh V (2015) Review Excitatory / Inhibitory Balance and Circuit Homeostasis in Autism Spectrum Disorders. Neuron 87:684–698.

Pappas SS, Leventhal DK, Albin RL, Dauer WT (2014) Mouse Models of Neurodevelopmental Disease of the Basal Ganglia and Associated Circuits. Curr Top Dev Biol 109:97–169.

Paraskevopoulou F, Herman MA, Rosenmund C (2019) Glutamatergic innervation onto striatal neurons potentiates GABAergic synaptic output. J Neurosci. 10.1523/JNEUROSCI.2630-18.2019.

Park H, Poo MM (2013) Neurotrophin regulation of neural circuit development and function. Nat Rev Neurosci 14:7–23.

Penrod RD, Campagna J, Panneck T, Preese L, Lanier LM (2015) The presence of cortical neurons in striatal-cortical co-cultures alters the effects of dopamine and BDNF on medium spiny neuron dendritic development. Front Cell Neurosci 9:1–14.

Ramamoorthi K, Lin Y (2011) The contribution of GABAergic dysfunction to neurodevelopmental disorders. Trends Mol Med 17:452–462.

Randall FE, Garcia-Munoz M, Vickers C, Schock SC, Staines WA, Arbuthnott GW (2011) The Corticostriatal System in Dissociated Cell Culture. Front Syst Neurosci 5:1–7.

Rauskolb S, Zagrebelsky M, Dreznjak A, Deogracias R, Matsumoto T, Wiese S, Erne B, Sendtner M, Schaeren-Wiemers N, Korte M, Barde Y-A (2010) Global Deprivation of Brain-Derived Neurotrophic Factor in the CNS Reveals an Area-Specific Requirement for Dendritic Growth. J Neurosci 30:1739–1749.

Rutherford LC, Dewan A, Lauer HM, Turrigiano GG (1997) Brain-Derived Neurotrophic Factor Mediates the Activity- Dependent Regulation of Inhibition in Neocortical Cultures. J Neurosci 17:4527–4535.

Segal M, Greenberger V, Korkotian E (2003) Formation of dendritic spines in cultured striatal neurons depends on excitatory afferent activity. Eur J Neurosci 17:2573–2585.

Seil FJ, Drake-Baumann R (1994) Reduced Cortical Inhibitory Synaptogenesis in Organotypic Cerebellar Cultures Developing in the Absence of Neuronal Activity. J Comp Neurol 342:366–377.

Seil FJ, Drake-Baumann R (2000) TrkB Receptor Ligands Promote Activity-Dependent Inhibitory Synaptogenesis. J Neurosci 20:5367–5373.

Shepherd GMG, Katz DM (2011) Current Opinion in Neurobiology. Curr Opin Neurobiol 21:827–833.

Smith Y, Raju D, Nanda B, Pare J, Galvan A, Wichmann T (2009) The Thalamostriatal Systems: Anatomical and Functional Organization in Normal and Parkinsonian States. Brain Res Bull 78:60–68.

Smith Y, Raju D V, Pare JF, Sidibe M (2004) The thalamostriatal system: A highly specific network of the basal ganglia circuitry. Trends Neurosci 27:520–527.

Stern E a, Kincaid a E, Wilson CJ (1997) Spontaneous subthreshold membrane potential fluctuations and action potential variability of rat corticostriatal and striatal neurons in vivo. J Neurophysiol 77:1697–1715.

Surmeier DJ, Ding J, Day M, Wang Z, Shen W (2007) D1 and D2 dopamine-receptor modulation of striatal glutamatergic signaling in striatal medium spiny neurons. Trends Neurosci 30:228–235.

Taverna S, Ilijic E, Surmeier DJ (2008) Recurrent collateral connections of striatal medium spiny neurons are disrupted in models of Parkinson's disease. J Neurosci 28:5504–5512.

Thoenen H (1995) Hans Thoenen. Science (80-) 270:593–598.

Vicario-abejo C, Collin C, Mckay RDG, Segal M (1998) Neurotrophins Induce Formation of Functional Excitatory and Inhibitory Synapses between Cultured Hippocampal Neurons. J Neurosci 18:7256–7271.

Vicario-abejón C, Owens D, Mckay R, Segal M (2002) Role of neurotrophins in central synapse formation and stabilization. Nat Rev Neurosci 3:965–974.

Vonsattel JP, DiFiglia M (1998) Huntington Disease. J Neuropathol Exp Neurol 57:369–384.

Wilson CJ (1993) The generation of natural firing patterns in neostiatal neurons. Prog Brain Res 99:277–297.

Wilson CJ (2014) The Sensory Striatum. Neuron 83:999–1001.

Zuccato C, Ciammola A, Rigamonti D, Leavitt BR, Goffredo D, Conti L, MacDonald ME, Timmusk T, Sipione S, Cattaneo E (2001) Loss of Huntingtin-Mediated BDNF Gene Transcription in Huntington ' s Disease. Science (80-) 293:493–498.

Affidavit

I, Foteini Paraskevopoulou, certify under penalty of perjury by my own signature that I have submitted the thesis on the topic ‘Investigation of striatal GABAergic output modulation by glutamatergic input’. I wrote this thesis independently and without assistance from third parties, I used no other aids than the listed sources and resources.

All points based literally or in spirit on publications or presentations of other authors are, as such, in proper citations (see "uniform requirements for manuscripts (URM)" the ICMJE www.icmje.org) indicated. The section on methodology (in particular practical work, laboratory requirements, statistical processing) and results (in particular images, graphics and tables) corresponds to the URM (s.o) and are answered by me. My contribution in the selected publication for this dissertation corresponds to those that are specified in the following joint declaration with the responsible person and supervisor.

The importance of this affidavit and the criminal consequences of a false affidavit (section 156,161 of the Criminal Code) are known to me and I understand the rights and responsibilities stated therein.

Date _____ Signature_____

Detailed Declaration of Contribution

Foteini Paraskevopoulou had the following share in the following publication:

Paraskevopoulou, F., Herman, M.A., Rosenmund, C. (2019). Glutamatergic innervation onto striatal neurons potentiates GABAergic synaptic output. *Journal of Neuroscience*, 10.1523/JNEUROSCI.2630-18.2019.

Contribution in detail:

Design of research:

M.A. Herman, C. Rosenmund and F. Paraskevopoulou conceived the idea and designed the experiments.

Execution of experiments and data analysis:

F. Paraskevopoulou performed all experiments including whole-cell patch-clamp recordings, immunocytochemistry, microscopy and qPCRs. R. Dannenberg and M. Petzold helped with the preparation of cell cultures. B. Söhl-Kielczynski helped with immunocytochemistry assay. Analyses for all experiments were carried out by F. Paraskevopoulou.

Manuscript preparation:

F. Paraskevopoulou interpreted the results with input from M.A. Herman and C. Rosenmund. F. Paraskevopoulou wrote the manuscript and prepared the figures. M.A. Herman and C. Rosenmund edited the manuscript. All authors approved the final manuscript.

Signature, date and stamp of the doctoral supervisor

_____

Signature of the doctoral candidate

_____

Excerpt from the Journal Summary List (ISI Web of Knowledge)

Journal Data Filtered By: **Selected JCR Year: 2017** Selected Editions: SCIE,SSCI
Selected Categories: **"NEUROSCIENCES"** Selected Category Scheme: WoS
Gesamtanzahl: 261 Journale

Rank	Full Journal Title	Total Cites	Journal Impact Factor	Eigenfactor Score
1	NATURE REVIEWS NEUROSCIENCE	40,834	32.635	0.069940
2	NATURE NEUROSCIENCE	59,426	19.912	0.153710
3	ACTA NEUROPATHOLOGICA	18,783	15.872	0.041490
4	TRENDS IN COGNITIVE SCIENCES	25,391	15.557	0.040790
5	BEHAVIORAL AND BRAIN SCIENCES	8,900	15.071	0.010130
6	Annual Review of Neuroscience	13,320	14.675	0.016110
7	NEURON	89,410	14.318	0.216730
8	PROGRESS IN NEUROBIOLOGY	13,065	14.163	0.015550
9	BIOLOGICAL PSYCHIATRY	42,494	11.982	0.056910
10	MOLECULAR PSYCHIATRY	18,460	11.640	0.047200
11	JOURNAL OF PINEAL RESEARCH	9,079	11.613	0.008600
12	TRENDS IN NEUROSCIENCES	20,061	11.439	0.026860
13	BRAIN	52,061	10.840	0.075170
14	SLEEP MEDICINE REVIEWS	6,080	10.602	0.010720
15	ANNALS OF NEUROLOGY	37,251	10.244	0.053390
16	Translational Stroke Research	2,202	8.266	0.005260
17	NEUROSCIENCE AND BIOBEHAVIORAL REVIEWS	24,279	8.037	0.048460
18	NEUROSCIENTIST	4,738	7.461	0.008730
19	NEURAL NETWORKS	10,086	7.197	0.015290
20	FRONTIERS IN NEUROENDOCRINOLOGY	3,924	6.875	0.006040
21	NEUROPSYCHOPHARMACOLOGY	24,537	6.544	0.042870
22	CURRENT OPINION IN NEUROBIOLOGY	14,190	6.541	0.034670
23	Molecular Neurodegeneration	3,489	6.426	0.009850
24	CEREBRAL CORTEX	29,570	6.308	0.058970
25	BRAIN BEHAVIOR AND IMMUNITY	12,583	6.306	0.026850
26	BRAIN PATHOLOGY	4,952	6.187	0.007750
27	Brain Stimulation	4,263	6.120	0.014510
28	NEUROPATHOLOGY AND APPLIED NEUROBIOLOGY	3,654	6.059	0.006350
29	JOURNAL OF CEREBRAL BLOOD FLOW AND METABOLISM	19,450	6.045	0.028280
30	JOURNAL OF NEUROSCIENCE	176,157	5.970	0.265950
31	Molecular Autism	1,679	5.872	0.006320
31	Translational Neurodegeneration	589	5.872	0.002280
33	GLIA	13,417	5.846	0.020530
34	Neurotherapeutics	3,973	5.719	0.008980
35	PAIN	36,132	5.559	0.038000
36	NEUROIMAGE	92,719	5.426	0.152610
37	Acta Neuropathologica Communications	2,326	5.414	0.011550
38	Multiple Sclerosis Journal	10,675	5.280	0.021890

Printed copy of selected publication

Paraskevopoulou, F., Herman, M.A., Rosenmund, C. (2019). Glutamatergic innervation onto striatal neurons potentiates GABAergic synaptic output. *Journal of Neuroscience*, 10.1523/JNEUROSCI.2630-18.2019

JNeurosci
THE JOURNAL OF NEUROSCIENCE

Research Articles: Cellular/Molecular

Glutamatergic innervation onto striatal neurons potentiates GABAergic synaptic output

Foteini Paraskevopoulou[1], Melissa A. Herman[1] and Christian Rosenmund[1]

[1]*Department of Neurophysiology, NeuroCure Cluster of Excellence, Charité Universitätsmedizin, 10117 Berlin, Germany*

https://doi.org/10.1523/JNEUROSCI.2630-18.2019

Received: 11 October 2018

Revised: 24 March 2019

Accepted: 26 March 2019

Published: 1 April 2019

Author contributions: F.P., M.H., and C.R. designed research; F.P. performed research; F.P. analyzed data; F.P. wrote the paper; M.H. and C.R. edited the paper.

Conflict of Interest: The authors declare no competing financial interests.

F.P. was funded by a pre-doctoral fellowship from NeuroCure Cluster of Excellence. This work was funded by Neurocure Excellence Initiative and the German Research Council (Deutsche Forschungsgemeinschaft; SFB665/B11 to CR; HE 7480/2-1 to MH). We thank Bettina Brokowski, Rike Dannenberg, Berit Söhl-Kielczynski, Miriam Petzold and Katja Pötschke, for technical assistance and members of the Rosenmund laboratory for discussions.

Correspondence: Christian Rosenmund at Department of Neurophysiology, NeuroCure Cluster of Excellence, Charité Universitätsmedizin, 10117 Berlin, Germany

Cite as: J. Neurosci 2019; 10.1523/JNEUROSCI.2630-18.2019

Glutamatergic innervation onto striatal neurons potentiates GABAergic synaptic output

Foteini Paraskevopoulou[1], Melissa A. Herman[1], Christian Rosenmund[1*]

[1]Department of Neurophysiology, NeuroCure Cluster of Excellence, Charité Universitätsmedizin, 10117 Berlin, Germany

Abbreviated title: Glutamatergic input modulates striatal output

Author contributions: F.P. performed experiments, analyzed data and wrote the manuscript; F.P, M.A.H. and C.R. designed research; M.A.H. and C.R. edited the manuscript.

***Correspondence**: Christian Rosenmund at Department of Neurophysiology, NeuroCure Cluster of Excellence, Charité Universitätsmedizin, 10117 Berlin, Germany

Email: christian.rosenmund@charite.de.

Number of pages: 45

Number of figures: 5

Number of tables: 0

Number of extended data: 5

Number of words for Abstract: 243

Number of words for Introduction: 649

Number of words for Discussion: 1411

Conflict of Interest: The authors declare no competing financial interests.

Acknowledgements: F.P. was funded by a pre-doctoral fellowship from NeuroCure Cluster of Excellence. This work was funded by Neurocure Excellence Initiative and the German Research Council (Deutsche Forschungsgemeinschaft; SFB665/B11 to CR; HE 7480/2-1 to MH). We thank Bettina Brokowski, Rike Dannenberg, Berit Söhl-Kielczynski, Miriam Petzold and Katja Pötschke, for technical assistance and members of the Rosenmund laboratory for discussions.

Abstract

Striatal output pathways are known to play a crucial role in the control of movement. One possible component for shaping the synaptic output of striatal neuron is the glutamatergic input that originates from cortex and thalamus. Although, reports focusing on quantifying glutamatergic-induced morphological changes in striatum exist, the role of glutamatergic input in regulating striatal function remains poorly understood. Using primary neurons from newborn mice of either sex in a reduced two-neuron microcircuit culture system, we examined whether glutamatergic input modulates the output of striatal neurons. We found that glutamatergic input enhanced striatal inhibition, *in vitro*. With either a glutamatergic partner from cortex or thalamus, we attributed this potentiation to an increase in the size of quantal IPSC, suggesting a strengthening of the postsynaptic response to GABAergic signaling. Additionally, a differential effect of cortical and thalamic innervation onto striatal GABAergic neurons output was revealed. We observed that cortical, but not thalamic input, enhanced the number of releasable GABAergic synaptic vesicles and morphological synapses. Importantly, these alterations were reverted by blockade of neuronal activity and glutamate receptors, as well as disruption of BDNF-TrkB signaling. Together, our data indicate for first time that GABAergic synapse formation in cortico-striatal pairs depends on two parallel, but potentially intersecting, signaling pathways that involve glutamate receptor activation in striatal neurons, as well as BDNF signaling. Understanding how cortical and thalamic inputs refine striatal output will pave the way towards dissecting basal ganglia activity in both physiological and pathological conditions.

Key words: striatum, GABAergic neurons, synaptic output, two-neuron microcircuit, glutamatergic input, BDNF, autapses, paired recordings

Significance statement

Striatal GABAergic microcircuits are critical for motor function. However, the mechanisms controlling striatal output, particularly at the level of synaptic strength, are unclear. Using two-neuron culture system, we quantified the synaptic output of individual striatal GABAergic neurons paired with a glutamatergic partner and studied the influence of the excitatory connections that are known to be inter-regionally formed *in vivo*. We found that glutamatergic input potentiated striatal inhibitory output, potentially involving an increased feedback and/or feed-forward inhibition. Moreover, distinct components of glutamatergic innervation, such as firing activity or release of neurotrophic factors were shown to be required for the glutamatergic-induced phenotype. Investigation, therefore, of two-neuron *in vitro* microcircuits could be a powerful tool to explore synaptic mechanisms or disease pathophysiology.

Introduction

The striatum is a unique structure containing a high density of GABAergic projection neurons. It serves as the primary gateway for glutamatergic input to the basal ganglia, and its inhibitory output is associated primarily with motor function (Albin et al., 1989; DeLong, 1990). Based on previous *in vivo* studies, ~95% of striatal neurons are spiny (medium spiny neurons; MSNs) and interconnected by local recurrent axon collateral synapses (Czubayko and Plenz, 2002; Tunstall et al., 2002). The MSNs project within basal ganglia networks, such as globus pallidus, and substantia nigra, through direct and indirect output pathways (Albin et al., 1989; Gerfen, 1992). In recent years, much attention has been drawn toward unveiling the role of striatal projection neuron output in movement (Cui et al., 2013; Oldenburg and Sabatini, 2015; Rothwell et al., 2015), but despite the advances in our understanding of basal ganglia circuitry, mechanisms controlling striatal output, particularly at the level of synaptic strength, are still far from clear.

One possible component for shaping the output of striatal neuron synapses is the glutamatergic input onto the neurons themselves. Glutamatergic innervation into striatum mainly originates from cerebral cortex (Kemp and Powell, 1970; McGeorge and Faull, 1989) and thalamus (Groenewegen and Berendse, 1994; Salin and Kachidian, 1998). In particular, motor cortex gives rise to massive excitatory projections that end at the striatum and provide the striatum with information necessary to control motor behavior (Gerfen, 1992; Wilson, 2014). In parallel, thalamic nuclei projections target sensorimotor striatal regions and influence the processing of functionally segregated information (Smith et al., 2004). Previous studies suggest that glutamatergic input not only provides

99 excitation to target GABAergic neurons, but also modulates the size of their inhibitory
100 output, particularly in interneurons through control of synapse formation (Chang et al.,
101 2014). If such modulation is also present at striatal GABAergic neurons, it could have the
102 potential to affect the balance of direct and indirect striatal projections, the strength of
103 lateral inhibition through recurrent connections within striatum, and hence general basal
104 ganglia function.

105 In the past, efforts have been made to decipher how cortico- and thalamo-striatal
106 projections modulate striatal circuit activity and MSN excitability (Wilson, 1993; Ding et
107 al., 2008). It has been shown *in vivo* that cortical activity is correlated with MSN
108 transitions from inactive or hyperpolarized to depolarized states, suggesting that
109 prolonged depolarizations are determined by sustained excitatory activity (Stern et al.,
110 1997). Additionally, experiments in acute mouse brain slice revealed that glutamatergic
111 afferents projecting from cortex and thalamus exhibit different short-term synaptic
112 plasticity properties, promoting distinct patterns of MSN spiking (Ding et al., 2008).
113 Although these studies yielded valuable insights, innate technical problems prevent the
114 ability to identify the role of glutamatergic input in regulating striatal activity and to
115 quantify the synaptic output of individual striatal neurons. Dissociated *in vitro* cell
116 culture systems are at present the most efficient method for recording pairs (Randall et
117 al., 2011) and quantifying the input and output of individual striatal neurons.

118 In the present study, we used an *in vitro* dissociated two-neuron inter-regional
119 microcircuit to explore whether glutamatergic input from cortex or thalamus affects the
120 output of individual striatal GABAergic projection neurons. We recorded connected
121 neurons and evaluated the number of synaptic contacts involved in striatal transmission

and identified the synaptic properties of all the possible connections. Furthermore, we explored the contributions of distinct components of glutamatergic innervation, such as introduction of activity or release of brain derived neurotrophic factor (BDNF), both of which are crucial for GABAergic synapse formation and function (Hartman et al., 2006; Park and Poo, 2013; Chang et al., 2014). We found that glutamatergic input onto striatal GABAergic neurons did indeed modulate inhibitory synaptic transmission by regulating their output. This process was dependent on action potential generation, glutamatergic synaptic transmission and BDNF secretion. Together these results provide insights into basal ganglia physiology and suggest molecular mechanisms through which glutamatergic input modulates striatal output pathways in healthy brain.

Materials and methods

Mice and cell culture

Animal housing and use were in compliance with and approved by the Animal Welfare Committee of Charité Medical University and the Berlin State Government Agency for Health and Social Services (License T0220/09). Newborn C57BLJ6/N mice (P0-P2) of both sexes were used for all the experiments.

Primary neurons were seeded and cultured on microisland astrocyte feeder layers that were prepared 2 weeks before the neuronal culture preparation. Astrocytes derived from C57BL6/N mouse cortices (P0-P1) were plated on collagen/ poly-D-lysine microislands made on agarose-coated coverslips using a custom-built rubber stamp to achieve uniform size (200µm diameter). For all experiments, neurons from striatum,

cortex or thalamus were digested with papain (Worthington), mechanically dissociated, and plated on astrocytes in a chemically defined medium (Neurobasal-A medium supplemented with Glutamax and B-27; Invitrogen, Germany). For two-neuron cultures, neurons were plated at 1:1 ratio and at a total density of $1x10^4$ neurons per 35 mm well. For mass cultures used for qPCR, neurons were plated in absence of astrocytic layer at a density of $5x10^5$-$6x10^5$ neurons per 35 mm well.

For drug treatment experiments, neurons were treated with 0.5 µM tetrodotoxin (TTX; Tocris Bioscience); 2 µM 2,3-dihydroxy-6-nitro-7-sulfamoyl-benzo[f]quinoxaline-2,3-dione (NBQX; Tocris Bioscience) and 100 µM d-(-)-2-amino-5-phosphonopentanoic acid (APV; Tocris Bioscience); 200 nM K252a (Tocris Bioscience); BDNF neutralizing antibody α-BDNF (1:100; Millipore) and human recombinant BDNF (50 ng/ml; Peprotech) at days *in vitro* (DIV) 3, 7, 11.

Membrane dye labeling

To identify the cell region of origin in electrophysiological recordings, dissociated tissues for the two-neuron cultures were labeled with different fluorescent membrane dyes (PKH26 red or PKH67 green) using a fluorescent cell linker kit for general membrane labeling (Sigma).

Electrophysiology

Paired whole-cell voltage-clamp recordings were performed with a Multiclamp 700B amplifier (Molecular Devices, Sunnyvale, CA) under the control of Clampex 10.2 (Molecular Devices) between DIV 12 –15. Data were digitally sampled at 10 kHz and

low-pass Bessel filtered at 3 kHz with an Axon Digidata 1440A digitizer (Molecular Devices). Series resistance was compensated at 70% and only cells with <12 MΩ resistance were included. All experiments were performed at room temperature (23–24°C).

During recordings, neurons were immersed in standard extracellular solution consisting of (in mM) of: 140 NaCl, 2.4 KCl, 10 HEPES, 10 glucose, 4 $MgCl_2$, and 2 $CaCl_2$. The patch pipette internal solution contained the following (in mM): 136 KCl, 17.8 HEPES, 1 EGTA, 0.6 MgCl2, 4 ATP-Mg, 0.3 GTP-Na, 12 phosphocreatine, and 50 U/ml phosphocreatine kinase. Both solutions were adjusted to pH 7.4 with osmolarity at 300 mOsm. Borosilicate glass patch pipettes were pulled using a multistep puller (P-87, Sutter Instruments) using conditions that kept pipette tip resistance between 2-5 MΩ.

Action potential evoked postsynaptic currents (PSCs) were triggered by a 2 ms somatic depolarization from -70mV (holding potential) to 0 mV. Neurons were stimulated at 0.1 Hz in standard external solution to measure basal evoked excitatory or inhibitory postsynaptic currents (EPSCs or IPSCs, respectively). The kinetics of the evoked responses and AMPA receptor antagonist (3 μM 2,3-dihydroxy-6-nitro-7-sulfamoyl-benzo[f]quinoxaline-2,3-dione (NBQX); Tocris Bioscience) were used in order to verify glutamatergic or GABAergic identities. Spontaneous release of GABAergic cells only, was determined by detecting miniature IPSCs (mIPSCs), in the presence of NBQX, for 20–40 s at −70 mV with the help of a template-based algorithm in Axograph X v1.6.4 (Axograph Scientific, Berkeley, CA). Data were filtered at 1kHz and the threshold for detection was set at three times the baseline SD from a template of 0.5 ms rise and 18 ms decay time for GABAergic events. Membrane capacitance

measurements were obtained from the membrane test function in pClamp (Molecular Devices). Readily releasable pool (RRP) size of striatal cells (GABAergic only) was assessed by measuring the charge transfer of the transient synaptic current induced by a 5 s application of 500 mM hypertonic sucrose in standard extracellular solution supplemented with NBQX (Rosenmund et al., 1996). The output RRP was the sum of the autaptic and heterosynaptic RRPs in mixed pairs (Glu-GABA). In the case of control striatal pairs (GABA-GABA), a configuration in which the contribution of each neuron's output RRP is not pharmacologically distinguishable, the output RRP was divided by half for each GABAergic neuron, assuming that both RRPs are of equal size. The number of synaptic vesicles in the RRP of neurons was calculated by dividing the sucrose charge by the charge of the average miniature event of the same neuron. Similarly, the release probability of a single synapse (Pvr) was calculated as the ratio of input evoked response charge (autaptic and heterosynaptic connections ending at each postsynaptic neuron) to output RRP charge of the same neuron. Short-term plasticity was examined either by evoking 50 synaptic responses at 5 Hz or 2 responses at 20 Hz (inter-stimulus interval of 50 ms) to calculate a paired-pulse ratio (PPR; response 2/ response 1). Data were analyzed in Axograph X (Axograph Scientific, Berkeley, CA), Excel (Microsoft, Redmond, WA) and Prism (GraphPad, La Jolla, CA). All experiments were performed blinded to the experimental groups and coverslips were always randomized to drug treatments in all experiments. Cells were excluded for further analysis when neither sponanteous release nor hypertonic sucrose-evoked release was detected.

Immunocytochemistry

At DIV12-15 (unless otherwise noted), neurons were rinsed with phosphate buffer saline (PBS) and fixed in 4% w/v paraformaldehyde in PBS, pH 7.4 for 10 min in room temperature, after which they were washed thrice in PBS. Following permeabilization and blocking with 5% v/v normal donkey serum (NDS) in PBS with 0.1% Tween (PBST) for 1 hr, cells were incubated with primary antibodies of interest overnight at 4 ^{0}C. We used the following antibody dilutions: (i) mouse anti-VGAT (1:1000; Synaptic Systems, Germany), (ii) chicken anti-microtubule-associated protein 2 (MAP2) (1:2000; Millipore), (iii) guinea pig anti-VGLUT1 (1:4000; Synaptic Systems) and (iv) guinea pig anti-VGLUT2 (1:1000; Synaptic Systems). Coverslips were then washed thrice with PBST for 15 min each and primary antibodies were labeled with secondary Alexa-Fluor 488, 555 or 647 (1:500; Jackson, West Groove, PA) antibodies for 1 hr at room temperature. Finally, coverslips were washed twice with PBST and twice with PBS for 15 min each after that they were mounted on glass slides with Mowiol.

Quantification of neuronal morphology

For morphological analysis, 16-bit images were acquired on an Olympus IX81 inverted epifluorescence microscope at 20x optical magnification with a CCD camera (Princeton MicroMax; Roper Scientific, Trenton, NJ) and MetaMorph software (Molecular Devices). At least three independent cultures were imaged and analyzed blindly to groups for every experiment. All images were acquired using equal exposure times and subjected to uniform background subtraction (radius of 30 pixels) and optimal threshold adjustment.

To determine total dendrite length, MAP2-positive processes were traced with the

NeuronJ plugin (Meijering et al., 2004) and cross-sectional area across the MAP2-positive cell body was measured to estimate the area of neuronal somata. For synapse number quantification, GABAergic synapses were identified by immunoreactivity to VGAT antibody, while glutamatergic synapses in coritico-straital pairs were identified by immunoreactivity to VGLUT1 antibody and glutamatergic synapses in thalmo-striatal pairs identified by immunoreactivity to VGLUT2 antibody according to the reported vesicular glutamate transporter isoform expression pattern (Fremeau et al., 2001; Fujiyama et al., 2001). The total number of GABAergic and glutamatergic synapses was quantified by manually counting the VGAT and VGLUT1 (cortex) or VGLUT2 (thalamus) fluorescent punta, respectively. After background subtraction with a rolling ball of a radius of 30 pixels and threshold adjustment, images were converted to binary using ImageJ plugin. Only puncta with less than 6 pixels^2 were included in the analysis. For heterotypic pairs, the total number of VGAT puncta represented all the synapses of the GABAergic partner, while in homotypic striatal pairs the same measure represented the synapses from both GABAergic cells. Therefore, the total number of VGAT puncta was divided by half, in the case of striatal pairs. Raw values were exported to Prism (GraphPad, La Jolla, CA) for further analyses.

Quantitative real-time RT-PCR

Total cellular RNA was extracted using QIAzol Lysis Reagent (Qiagen) reagent and followed by complementary DNA (cDNA) synthesis using M-MLV reverse transcriptase (Promega) and random hexanucleotides. The mRNA expression levels of each sample were normalized to tubulin (Tubb3) mRNA content. For detection of the amplification

products in *Tubb3* and *Bdnf* RT-PCR, we used SYBR Green dye-based PCR amplification (Thermo Fisher Scientific) and the QuantStudio 3 detection system (Applied Biosystems). The following sequence-specific primers (MWG Biotech, Ebersberg, Germany) were used: Tubb3 forward, 5'-GCGCATCAGCGTATACTACAA-3' and reverse, 5'-CATGGTTCCAGGTTCCAAGT-3'; Bdnf forward, 5'-GACGACATCACTGGCTGACA-3' and reverse, 5'-CAAGTCCGCGTCCTTATGGT-3'.

Statistical Analysis

Power analysis was performed using the pwr *R* package (https://github.com/heliosdrm/pwr) prior to experimental design in order to estimate the sample size for detecting differences, if exist, between conditions. A statistical power of 0.8 was set for pairwise comparisons, with a two-side type I error rate of 0.05 and a medium effect size of 0.5 (Cohen, 1988). To evaluate our methodological approach, at the end of the experiment the statistical power was recalculated (≥ 0.9 in all cases) using the empirical mean values of the compared groups, the standard deviation, the alpha and sample size. To test the normality of the data, we used the D'Agostino-Pearson test. Student's *t* test for independent groups and one-way ANOVA using Tukey *HSD* post-hoc test were used to assign the level of statistical significance between conditions. When parametric assumptions were violated, we performed Mann-Whitney U test and Kruskal-Wallis test coupled with Dunn's post hoc test. All analyses were carried out in Prism v.7. Data are presented as mean ± SEM.

Results

To investigate the interaction between excitatory (cortical or thalamic) and striatal inhibitory neurons on the cellular level, we utilized two-neuron microisland cultures. In each condition, we systematically altered the neuron type (glutamatergic or GABAergic) and the tissue origin (cortex/thalamus or striatum) of each neuron. The tissue origin of each cell was determined by membrane dye-labeling of dissociated neurons prior to plating (see Materials and Methods) and neurotransmitter type was determined by kinetics of the postsynaptic responses (Fig. 1). This *in vitro* approach allowed us for an unambiguous and quantitative electrophysiological (455 pairs) and morphological (191 pairs) characterization of synaptic connectivity and function of neurons of known identity.

Glutamatergic innervation onto striatal neurons increases GABAergic synaptic output

Synapses originating from cortical or thalamic neurons onto medium spiny neurons (MSNs) provide most of the excitatory glutamatergic input onto the striatum (Smith and Bolam, 1990; Doig et al., 2010). Hence, we decided to test for changes in synaptic connectivity and strength with the innervation of striatal GABAergic neurons with either of the two inputs. To do so, we used a two-neuron microcircuit culture system and compared control striatal (SS) (only GABAergic; homotypic) pairs to cortico-striatal (CS) or thalamo-striatal (TS) (glu-GABA; heterotypic) pairs (Fig.1 and Fig.1-1). Because in this configuration, each neuron forms a synaptic connection with its partner

306 (heterosynapses), as well as with itself (autapses), four distinct synaptic connections are
307 present in each pair (Fig. 1A-C). To demonstrate that all changes in GABAergic output
308 are specific to the presence of glutamatergic partner, we used single striatal neurons,
309 growing on glial islands, as a second control, and compared their properties to homotypic
310 GABA pairs.

311 First, we analyzed the impact of glutamatergic innervation on action-potential-
312 evoked inhibitory postsynaptic currents (IPSCs) generated by striatal GABAergic
313 neurons, by looking at the total autaptic and heterosynaptic responses. Both cells in each
314 pair configuration (Fig. 1 A-C) were measured simultaneously using whole-cell patch-
315 clamp of their somata, and subsequent brief depolarizations were applied to elicit an
316 action potential in either of the connected neurons. Striatal neurons paired with either a
317 cortical or thalamic glutamatergic partner revealed an approximately two-fold increase in
318 evoked IPSC total amplitude (CS: -21.14±3.12 nA, n=29, p=0.006; TS: -19.13±3.29 nA,
319 n=25, p=0.026, Kruskal-Wallis test), compared to those paired with another striatal
320 GABAergic neuron (SS IPSC: -10.51±1.23 nA, n=60) (Fig.1D-G). These findings
321 suggest that glutamatergic input increases the magnitude of GABAergic output of striatal
322 neurons.

323 The magnitude of the evoked IPSC depends on the number of fusion competent
324 vesicles (readily releasable pool, RRP), the efficiency of the calcium-triggered fusion of
325 synaptic vesicles (vesicular release probability, Pvr) and the postsynaptic response to the
326 release of an individual vesicle (quantal size) (del Castillo and Katz, 1954; Reim et al.,
327 2001). In order to determine which of these parameters underlie the increase in evoked
328 release of striatal neurons in mixed pairs, firstly, we looked at readily releasable vesicles

in the presence of the glutamate receptor antagonist, NBQX. When we measured RRP size by integrating the charge resulting from the pulsed application of hypertonic sucrose supplemented with NBQX, we found that the total RRP size in striatal neurons connected with glutamatergic neurons was increased by 67% for cortico-striatal and 102% for thalamo-striatal pairs compared to striatal neuron pairs (SS: -3.77±0.30 nC, n=54; CS: -6.30±0.62 nC, n=27, p=0.002; TS: -7.61±0.91 nC, n=24, p=0.001, Kruskal-Wallis test) (Fig. 1D-F and H). This suggests that the magnitude of the increase in the RRP was comparable to the increase seen in the IPSC (101% and 82% respectively). We next examined whether glutamatergic input affects the presynaptic release efficiency by calculating the probability of single vesicle to undergo exocytosis (Pvr; IPSC charge divided by sucrose-evoked charge) or the paired pulse ratio (PPR). Our data revealed no changes in Pvr and PPR (SS: 13.66±1.24%, n=48; CS: 11.64±1.79%, n=27, p=0.625; TS: 14.07±1.76%, n=24, p>0.999, Kruskal-Wallis test) (Fig. 1I-J), implying that glutamatergic input affects RRP size without altering presynaptic calcium-dependent release efficiency.

To assess quantal size, we analyzed spontaneous release events, or miniature inhibitory PSCs (mIPSCs). We noted that the mean mIPSC amplitude of striatal neurons in mixed pairs was significantly greater than controls by approximately 70% (SS: -44.31±3.04 pA, n=42; CS: -74.24±7.07 pA, n=38, p=0.002; TS: -79.17±8.16 pA, n=32, p=0.001, Kruskal-Wallis test), as was the mIPSC charge (SS: -838.10±68.96 fC, n=42; CS: -1379±129.2 fC, n=38, p=0.004; TS: -1454±172.5 fC, n=32, p=0.01, Kruskal-Wallis test) (Fig. 1K-O). To eliminate the possibility that the mIPSC increase in mixed pairs is due to the nature of postsynaptic responses in glutamatergic neurons, we compared the

mIPSC amplitudes recorded only in the striatal GABAergic neurons in both homotypic and mixed pairs. We found that the GABAergic mIPSCs recorded in striatal neurons (autaptic) were also significantly increased by approximately 65% (SS: -45.26±2.9 pA, n=49; CS: -75.32 ± 6.6 pA, n=41, p<0.0001; TS: -72.96 ± 11.44 pA, n = 15, p = 0.043, Kruskal-Wallis test), suggesting that glutamatergic input alters the striatal neuron's sensitivity to GABA itself and thus potentiates the collateral feedback inhibition. The frequency of inhibitory miniature events was not changed despite the presence of glutamatergic input (SS: 2.15±0.26 Hz, n=42; CS: 1.70±0.35 Hz, n=41, p=0.121; TS: 2.54±0.47 Hz, n=36, p>0.999, Kruskal-Wallis test) (Fig.1P). We then calculated the total number of vesicles in the RRP by dividing the total output RRP charge by the average charge of the miniature events from each neuron. Our analysis showed that the mean number of synaptic vesicles contained in the RRP of striatal neurons was significantly increased only in the case of cortico-striatal pairs by 91%, but not in that of thalamo-striatal (SS: 4445±362, n=35; CS: 8498±1700, n=16, p=0.04; TS: 5197±990, n=14, p>0.999, Kruskal-Wallis test) (Fig. 1Q). This suggests a differential effect of cortical and thalamic innervation in striatum, in a way that only cortical input causes an increase in the number of RRP vesicles, while the increased RRP size in thalamo-striatal connections reflects the post-synaptic effect as supported by increased mIPSC size.

Different connectivity patterns revealed between cortico-striatal and thalamo-striatal pairs

To gain a better insight into the differential effect of cortical and thalamic input onto striatal neurons, we analyzed the strength of synaptic connection in mixed pairs by

assessing the total excitatory output of glutamatergic partners (Fig. 1R-T). We noted that the total EPSC amplitude of cortical neurons was 52% greater than the thalamic one (CS: -9.78±1.53 nA, n=30; TS: -4.72±0.95 nA, n=25, p=0.006, Mann-Whitney test) (Fig. 1R,S). However, when applying the paired pulse stimuli, the response ratios were indistinguishable (CS: 0.98±0.05, n=30; TS: 1.06±0.09 nA, n=25, p=0.42, t test) (Fig.1T), indicating that the relatively higher output from the cortical neurons onto striatal GABAergic neurons was not due to higher release efficacy, but was likely caused by a higher number of synaptic connections.

Excitation of either neuron within a pair resulted in autaptic (dark color bars) and heterosynaptic (light color bars) evoked responses from each neuron (Fig. 1U,V). Glutamatergic neurons from cortex, in mixed pairs, evoked on average bigger autaptic versus heterosynaptic responses (CS autaptic: -6.07±1.04 nA; heterosynaptic: -3.71±0.70 nA, n=30, p=0.04, Mann-Whitney test), while thalamic partners showed comparable autaptic and heterosynaptic EPSC amplitudes (TS autaptic: -2.44±0.66 nA; heterosynaptic: -2.49±0.56 nA, n=25, p=0.984, Mann-Whitney test) (Fig. 1U). To investigate whether the change in striatal GABAergic output was general or target specific, we compared the autaptic and heterosynaptic connections of striatal neurons across the different groups (Fig. 1V). In accordance with previous findings from hippocampal interneurons (Liu et al., 2009, 2013; Chang et al., 2014), we found that autaptic responses of striatal GABAergic neurons were two-fold higher than heterosynaptic in homotypic pairs (SS autaptic: -7.51±0.99 nA; heterosynaptic: -3.01±0.41 nA, n=60, p<0.0001, Mann-Whitney test) (Fig. 1V). Interestingly, while the total IPSC output (autaptic and heterosynaptic) from striatal neurons was significantly

greater in the presence of either cortical or thalamic partner (Fig. 1G), the preference for autaptic connections was only preserved in thalamo-striatal connections (Fig. 1V). On the other hand, upon cortical innervation, striatal neurons showed a specific increase in heterosynaptic response (Figure 1V; $p = 0.0045$). This could imply a target specific modulation of striatal neuron output in the cortico-striatal microcircuit.

Cortical input increases the number of GABAergic synapses in striatal neurons

Our electrophysiological experiments indicated a differential effect of cortical and thalamic innervation on striatal neurons function. While we observed an increase in the magnitude of the RRP output size of striatal GABAergic neurons co-cultured with either glutamatergic partner, only striatal neuron paired with a cortical glutamatergic neuron exhibited an increase in the number of RRP vesicles (Fig. 1H,Q). The increase in RRP vesicles could be a result of either a higher number of vesicles per synapse or by an increase in the number of synapses. To determine the locus of RRP vesicle increase in striatal GABAergic neurons paired with a cortical glutamatergic neuron, we examined the morphology of two-neuron cultures immuno-labeled with antibodies against: i) the predominant subtype of vesicular glutamate transporter (VGLUT) in cortical or thalamic neurons, VGLUT1 or VGLUT2, respectively to mark glutamatergic synapses (Fremeau et al., 2001; Fujiyama et al., 2001), ii) VGAT to mark GABAergic synapses and iii) MAP2 to visualize dendrites. We quantified the number of VGAT positive puncta in mixed and control pairs, and found near doubling (187%) in the number of GABAergic synapses made by striatal neurons in cortico-striatal pairs, but not in thalamo-striatal pairs (103%), compared to control neurons (SS: 174.8±17.48, n=23; CS: 326.3±41.52, n=21,

p=0.009; TS: 175.4±17.72, n=26, p>0.999, Kruskal-Wallis test) (Fig. 2A, B and Fig. 2-1). This is consistent with our findings from electrophysiological analysis and suggests that the larger number of RRP vesicles of striatal GABAergic neurons in cortico-striatal pairs is largely due to an increase in the number of GABAergic synapses formed. Indeed, when we quantified the number of excitatory synapses, VGLUT1 positive puncta for cortico-striatal pairs or VGLUT2 positive puncta for thalmo-striatal pairs, we revealed a higher number of connections formed by cortical compared to thalamic partners (CS: 312.2±38.7, n=23; TS: 118.2±15.5, n=25, p<0.0001, Mann-Whitney test) (Fig. 2C). This increased input from the cortical partners may underlie the further expansion of inhibition by the striatal neuron in this pair configuration compared to the thalamo-striatal pairs.

We also noted that striatal neurons tended to have an increased membrane capacitance (Cm) when cultured with either glutamatergic cells, compared to control neurons (SS: 20.22±1.32 pF, n=58; CS: 24.75±2.32 pF, n=29, p=0.368; TS: 24.02±2.87 pF, n=24, p>0.999, Kruskal-Wallis test) (Fig. 2D). Plausibly, changes in membrane capacitance correspond to an increase in cell surface area, and thus indicate a stimulation of growth of GABAergic neurons by glutamatergic innervation.

Neuronal activity modulates GABAergic synapse formation and function in cortico-striatal pairs

To gain mechanistic insight into how glutamatergic innervation drives the morpho-physiological changes in striatal GABAergic output, we went on to characterize the factors responsible for changes induced in the striatal neurons only in cortico-striatal pairs. We first investigated the role of neuronal activity (Fig.3 and Fig. 3-1). To do so, we

chronically inhibited neuronal activity in cortico-striatal cultures with tetrodotoxin (0.5 µM TTX) to block neuronal firing or glutamate receptor antagonists (2 µM NBQX, 100 µM AP5) to block postsynaptic receptor activation, applied to the culture media at DIV 3, 7, 11. We found that the IPSC amplitude in TTX-treated cortico-striatal pairs was reduced by 59% and in NBQX/APV-treated cortico-striatal pairs by 58%, compared to untreated cortico-striatal pairs (CS: -17.93±1.87 nA, n=37; CS+TTX: -7.34±1.25 nA, n=21, p=0.005; CS+NBQX/APV: -7.50±0.89 nA, n=18, p=0.041, Kruskal-Wallis test) (Fig. 3A). Likewise, RRP GABAergic size showed a significant decrease by 42% for TTX-treated cortico-striatal pairs and by 50% for NBQX/APV-treated cortico-striatal pairs (CS: -6.75±0.67 nC, n=37; CS+TTX: -3.88±0.66 nC, n=20, p=0.05; CS+NBQX/APV: -3.39±0.58 nC, n=19, p=0.008, Kruskal-Wallis test) (Fig. 3B). The release probability (Pvr) or short-term plasticity (PPR) characteristics as determined by paired pulse experiments were not significantly different after any drug application (Fig. 3C). Furthermore, we tested the effect of TTX or NBQX/APV treatment on the spontaneous release. In every case, chronic activity blockade effectively reversed the potentiation of mIPSC amplitudes upon cortical innervation back to control levels (CS: -77.56±4.51 pA, n=69; CS+TTX: -50.61±4.23 pA, n=34, p=0.001; CS+NBQX/APV: -54.62±5.15 pA, n=29, p=0.028, Kruskal-Wallis test) (Fig. 3D). The number of vesicles released onto striatal neurons in cortico-striatal pairs treated with TTX or NBQX/APV tended to be decreased back to the level of control striatal pairs (SS: 2740±450.7, n=34; CS: 5988±716.1, n=35; CS+TTX: 2963±451.9, n=19, p=0.187; CS+NBQX/APV: 2837±388.6, n=19, p=0.144, Kruskal-Wallis test) (Fig. 3E) as was true also for the membrane capacitance (SS: 19.3±1.24 pF, n=41; CS: 27.11±2.85 pF, n=39; CS+TTX:

17.5±1.87 pF, n=24, p=0.218; CS+NBQX/APV: 21.53±2.12 pF, n=17, p>0.999, Kruskal-Wallis test) (Fig. 3F). In general, control striatal pairs treated with either TTX or NBQX/APV did not show any significant differences, compared to the untreated controls. Overall, our results indicate that in cortico-striatal pairs, the GABAergic output is significantly shaped by action potential firing and associated glutamate release from the glutamatergic neuron.

BDNF elicits morphological differentiation of isolated striatal GABAergic neurons

In addition to providing excitatory neurotransmission to a circuit, glutamatergic neurons are also the source of other important factors, including brain derived neurotrophic factor (BDNF), which is crucial for GABAergic neuronal development (Park and Poo, 2013). In striatum, BDNF is considered to be released from glutamatergic synapses and not from the striatal MSNs themselves (Baydyuk and Xu, 2014). Given our findings that glutamatergic innervation stimulates formation of new synapse growth in GABAergic neurons, we investigated whether BDNF release from a cortical partner is involved in this growth.

First, we asked whether the application of BDNF alone is necessary and sufficient to induce the observed changes in striatal GABAergic output. We investigated the effects of BDNF on striatal GABAergic neuron morphology by chronically treating single striatal GABAergic neurons grown on microislands (autaptic culture) with BDNF (50 ng/ml at DIV 3,7,11) and performing immunocytochemical analysis at DIV 12-15 (Fig. 4). BDNF treatment resulted in a significant increase in growth of the striatal autaptic neurons. Particularly, soma size, VGAT positive puncta and dendritic length increased by

81% (control: 92.66±5.47 μm^2, n=40; BDNF: 168.1±9.21 μm^2, n=50, p<0.0001, Kruskal-Wallis test), 87% (control: 127.6±14, n=38; BDNF: 238.5±20.03, n=46, p=0.0001, Kruskal-Wallis test) and 75% (control: 714.3±62.08 μm, n=39; BDNF: 1251±93.45 μm, n=47, p<0.0001, Kruskal-Wallis test), respectively. This growth was fully reverted by an antagonist for BDNF receptors (tyrosine receptor kinase (Trk) antagonist; K252a 200nM at DIV 3,7,11) (BDNF+K252a soma: 122.9±6.80 μm^2, n=38, p=0.031; VGAT synapses: 120.3±10.72, n=39, p=0.0002; dendritic length: 783.7±73.33 μm n=44, p=0.0004, Kruskal-Wallis test) (Fig. 4A-D and Fig. 4-1A). In addition, we performed a series of experiments using the selective TrkB antagonist ANA12 (10 μM at DIV 3, 7, 11). However, due to irregular toxicity effects of ANA12 on the supporting astrocytes (over 80% of the astrocytic islands per culture were dissolved between the second and third dose at DIV 9-11; data not shown), we decided to only proceed with K252a. As an additional control experiment, to verify the specificity of BDNF-mediated morphological changes, we chronically treated the autaptic neurons with 50 ng/ml heat-inactivated BDNF (BDNF was heat inactivated by boiling for 5 min immediately before use at DIV3, 7, 11). Neurons treated with heat-inactivated BDNF revealed no changes in morphology (VGAT synapses control: 116.9±8.41, n=36; BDNF-heated: 122.9±10.8, n=39, p=0.948, Mann-Whitney test).

We next examined the functional implications of BDNF treatment on GABAergic output of single striatal autaptic neurons (Fig. 4-1B). Even though morphological analysis revealed a clear increase in the number of GABAergic synapses formed, BDNF treated neurons showed a 14% decrease in evoked IPSC amplitude (control: -6.84±0.63 nA, n=76; BDNF: -5.89±0.63 nA, n=127, p=0.013, Mann-Whitney test) (Fig. 4E), with no

significant difference in the RRP size (control: -3.13±0.29 nC, n=76; BDNF: -2.47±0.17 nC, n=127, p=0.092, Mann-Whitney test) (Fig. 4F). As there is no apparent change in release efficiency (Fig. 4G), the slight decrease in the autaptic IPSC amplitude likely reflects a smaller quantal size. Indeed, consistent with this scenario, there was a 22% decrease in mIPSC size (control: -50.12±2.87 pA, n=74; BDNF: -39.27±1.88 pA, n=120, p=0.0009, Mann-Whitney test), without any change in frequency, in BDNF-treated as compared to control neurons (Fig. 4H, J). One possible explanation for the decreased quantal size in BDNF-treated striatal autapses is that increased number of synapses formed is not accompanied by a concomitant increase in postsynaptic GABA receptors, and therefore the same number of receptors is diluted over more synapses. To test this possibility we compared the responses to exogenous GABA (5 μM) application and found that there was no difference between BDNF-treated and control neurons (control: 1±0.1, n=8; BDNF: 0.97±0.09, n=10, p=0.834, t test) (Fig. 4K), even though the BDNF-treated neurons have a significantly increased membrane capacitance (control: 17.78±1.06 pF, n=77; BDNF: 21.69±0.90 pF, n=128, p=0.0005, Mann-Whitney test) (Fig. 4L), and thus increased membrane surface area. This suggests that while BDNF, in the absence of glutamatergic excitatory transmission, is able to induce synapse formation, it does not support an increase in functional postsynaptic GABA receptors mirroring the presynaptic changes.

Activity-dependent endogenous BDNF release modulates GABAergic synapse formation and function in cortico-striatal pairs

We have shown separately that glutamatergic excitatory transmission in cortico-striatal two-neuron microcircuit evokes changes in striatal GABAergic output (Fig. 3) and that exogenous application of BDNF to isolated striatal GABAergic neurons promotes synapse formation (Fig. 4). However, is activity-dependent BDNF release from the cortical neuron driving the changes that observed in the striatal GABAergic neurons in cortico-striatal pairs? We first investigated whether, in our culture system, the source of BDNF is in fact the glutamatergic inputs and not the striatal GABAergic neurons. To this end, we compared mRNA levels using real time PCR from pure cultures of dissociated cortex or striatum. In agreement with previous findings examining BDNF mRNA levels (Conner et al., 1997; Gharami et al., 2008), we found that the BDNF mRNA was twice as high in cortical versus striatal cultures (cortical 197±26% of striatal, n=3, p=0.029, Mann-Whitney test) (Fig. 5A), indicative of the glutamatergic inputs as a potential source of BDNF.

To test if BDNF released from glutamatergic neurons is required for the observed changes in striatal GABAergic output, we disrupted the BDNF-TrkB receptor signaling pathway in cortico-striatal and striatal only pairs (Fig. 5). We found that chronically inhibiting TrkB receptors, using the Trk inhibitor K252a, reverted the IPSC by 25% (SS: -5.21±0.89 nA, n=44; CS: -10.38±1.23 nA, n=54, p=0.007; CS+K252a: -7.73±1.47 nA, n=32, p=0.042, Kruskal-Wallis test) and the RRP by 40% in cortico-striatal pairs (SS: -2.29±0.26 nC, n=37; CS: -4.58±0.37 nC, n=49, p<0.0001; CS+K252a: -2.74±0.38 nC, n=31, p=0.003, Kruskal-Wallis test) (Fig. 5B,C), back to the level of those parameters measured in striatal only pairs. Similar changes were observed for mIPSC events, where K252a inhibition caused a 30% reduction in amplitude (SS: -42.96±2.58 pA, n=40; CS: -

66.59±4.64 pA, n=63, p=0.013; CS+K252a: -46.82±3.55 pA, n=58, p=0.009, Kruskal-Wallis test) (Fig. 5E). Importantly, K252a treatment in striatal only pairs induced no changes in neurotransmission (Fig. 5B-H and Fig. 5-1), verifying the glutamatergic cortical neurons as the source of endogenous BDNF. The same findings were also confirmed by morphological analysis of pairs immunolabeled for the presynaptic marker VGAT (Fig, 5J-K). Cortico-striatal pairs treated with K252a antagonist revealed 46% reduction in inhibitory synapses, compared to the untreated pairs (CS: 498.5±63.2, n=32; CS+K252a: 269.3±30.89, n=29, p=0.048, Kruskal-Wallis test).

To further investigate the specificity of endogenous BDNF release and support the involvement of the BDNF-TrkB signaling pathway in regulation of striatal synapse formation, we chronically treated cortico-striatal pairs with anti-BDNF neutralizing antibody (1:100 at DIV3, 7, 11). BDNF neutralization led to a 60% decrease in inhibitory synapses of cortico-striatal pairs, compared to untreated heterotypic pairs (CS: 498.5±63.2, n=32; CS+anti-BDNF: 197.7±22.99, n=33, p<0.0001, Kruskal-Wallis test), thereby negating the cortical input-induced phenotype. Additionally, the number of excitatory synapses from cortical partner was reduced by 45% (CS: 570.6±52.46, n=35; CS+anti-BDNF: 314.8±29.01, n=33, p=0.001, Kruskal-Wallis test). Together, this provides evidence that abolishing endogenous BDNF function can affect inhibitory synapse formation in striatal neurons either directly through BDNF release or by decreasing excitatory synaptic contacts and thus the level of excitation.

Overall, these data suggest that glutamatergic firing, postsynaptic glutamate receptor activation and activity-dependent BDNF release potentiate the formation of GABAergic synapses in the cortico-striatal system.

Discussion

Our study investigates the potential role of glutamatergic innervation in shaping functional and morphological properties of striatal GABAergic neurons. Using a minimal circuit consisting of two neurons, we provide novel information regarding the impact of the cortical and thalamic glutamatergic input on the output synapses of the striatal GABAergic neurons. First, we report that glutamatergic input causes a two-fold increase in striatal GABAergic output. With both glutamatergic partners from cortex or thalamus, we attribute this potentiation to an increase in the postsynaptic response to GABA release. Additionally, we found that cortical, but not thalamic input, enhanced the number of inhibitory synapses formed by striatal GABAergic neurons, likely as a result of the higher number of synaptic contacts that cortical neurons formed over their striatal partners. Importantly, both alterations were reverted by inhibition of neuronal activity and glutamate receptors, as well as BDNF-TrkB signaling disruption. Together, our data indicate that GABAergic synapse formation in cortico-striatal pairs depends on two parallel, but potentially intersecting, signaling pathways that involve ionotropic glutamate receptor and BDNF-mediated signaling activation in striatal neurons.

Cortical and thalamic glutamatergic neurons increase striatal GABAergic output

Glutamatergic innervation from neocortex and thalamus is known to be a powerful modulator of dendritic morphology in MSNs (Segal et al., 2003; Buren et al., 2016). However, the effects of cortical and thalamic inputs on the physiology of striatal GABAergic neurons are currently understudied. Here, we denote for the first time that

glutamatergic input from either cortex or thalamus onto striatal neurons significantly increased total GABAergic synaptic output (Fig. 1). This finding partially agrees with previous studies in the hippocampus (Chang et al., 2014; Barrows et al., 2017) that reported an increase in GABAergic output upon glutamatergic innervation, suggesting a more general role of glutamatergic input in modulating the degree of inhibition produced by GABAergic neurons. Nevertheless, the modulation by glutamatergic input in the different types of GABAergic neurons manifests in different ways: hippocampal interneurons increased the number of their output synapses, but decreased the presynaptic release efficiency (Chang et al., 2014), whereas striatal GABAergic neurons increased their evoked inhibitory response and vesicle pool size, while maintaining their release efficiency (Fig. 1G-I). A possible explanation for this discrepancy might derive from the role of each GABAergic neuronal type within its given circuitry. Interneurons are thought to function mainly locally within a circuit and their output determines the excitation/inhibition balance (Liu, 2004; Atallah and Scanzianni, 2009). On the other hand, striatal neurons project to other regions and must reliably convey information (Kreitzer and Malenka, 2008). It is, thus, possible that striatal neurons are optimized to be less dynamic and rather act as refiners of incoming information from other neurons. Indeed, *in vivo* studies of the pathways from cortex and thalamus through striatum to the downstream areas suggest that the precision of striatal neuron firing is crucial for correct representation of sensory stimulus (Smith et al., 2004; Ding et al., 2008). Our findings that striatal GABAergic neurons respond to glutamatergic input with enhanced postsynaptic response to GABA release (Fig. 1N) would support this concept. Within the striatum, direct and indirect pathway MSNs communicate with each other via local axon

627 collaterals forming recurrent inhibitory synaptic contacts (Taverna et al., 2008). Given
628 our finding that glutamatergic innervation causes and increase in the quantal GABA
629 response on striatal neurons (Fig. 1), this would suggest that collateral recurrent
630 connections within striatum could be potentiated and therefore cause more precisely-
631 timed firing in response to excitatory input. The different properties of the two classes of
632 GABAergic neurons should come as no surprise, since interneurons and projection
633 neurons originate from different brain areas (medial and caudal *vs* lateral ganglionic
634 eminence, respectively) (Angevine and Sidman, 1961; Wichterle et al., 1997; Fjodorova
635 et al., 2015). This provides the two neuronal types with distinct transcriptional profiles
636 and thus, functional and morphological phenotypes.

637 Another interesting observation of our study is that thalamic and cortical inputs
638 differentially affect the cellular phenotype of striatal GABAergic output. Even though,
639 both glutamatergic inputs increased postsynaptic response of striatal GABAergic neurons
640 to GABA release (Fig. 1N), expansion of GABAergic output synapses occurred only with
641 cortical input (Fig. 1N, 2B). Cortico-striatal and thalamo-striatal projection systems code
642 information in distinct ways. This could constrain the way they regulate striatal circuitry
643 (Ding et al., 2008; Sciamanna et al., 2015) and thus, influence its output. Given that
644 BDNF impacts the formation of GABAergic synapses (Park and Poo, 2013), we
645 compared *Bdnf* mRNA levels between cortical and thalamic mass cultures. Yet, we found
646 no differences (data not shown). However, in morphological analysis of our pairs, the
647 number of cortical synapses made in cortico-striatal pairs was higher than those in
648 thalamo-striatal pairs (Fig. 2C). Therefore, we presume that the explanation for the
649 divergent effects of cortical versus thalamic input on striatal output stems from the

overall strength of the synaptic input provided by each of the glutamatergic partners. Indeed, in agreement with other studies (Smeal et al., 2007; Kolodziejczyk and Raymond, 2016), we found that, in addition to showing morphologically fewer synapses, thalamic neuron-evoked responses were smaller compared to those evoked by cortical neurons (Fig. 1R-S). This suggests that only strong synaptic input driven by cortical neurons might be able to induce the formation of additional inhibitory synapses in striatal GABAergic neurons.

Cortical-induced potentiation of striatal GABAergic output requires neuronal activity and activity-dependent BDNF release

The mechanisms through which striatal GABAergic neurons respond to glutamatergic innervation are currently unclear. We know from previous studies that excitation and activation of ionotropic glutamate receptors regulate GABAergic synapse formation in interneurons (Hartman et al., 2006; Chang et al., 2014). Furthermore, Segal et al. (2003) showed that in cortico-striatal embryonic cultures the presence of TTX in growth media prevented the increase in the density of striatal spines caused by cortical input. In this sense, our study verifies the importance of neuronal firing and glutamate receptor activation for GABAergic neuronal function, showing now that glutamatergic excitation not only alters striatal spines density, but it is also relevant for modulating GABAergic output (Fig. 3).

Another potential component of cortical glutamatergic innervation that impacts GABAergic output is activity-dependent BDNF release (Huang et al., 1999; Hong et al., 2008). In this context, we showed that the source of BDNF more likely comes from

673 glutamatergic fibers, as *Bdnf* mRNA expression was substantially higher in cortical than
674 striatal mass culture (Fig. 5A). Furthermore, we demonstrated for the first time that
675 application of Trk receptor antagonist, K252a, prevented the increase in GABAergic
676 output caused by cortical input, suggesting that BDNF is required for both quantal
677 response changes and inhibitory synapse formation (Fig. 5). This was also supported by
678 the experiments using anti-BDNF neutralizing antibody (Fig. 5J-K). This extends
679 previous findings on the role of BDNF as a regulator of cellular and dendritic
680 morphology for striatal GABAergic neurons (Nakao et al., 1995; Palizvan et al., 2004;
681 Rauskolb et al., 2010; Penrod et al., 2015). Nevertheless, despite the fact that BDNF
682 directly influences the morphology (cell size, dendritic length and number of contacts),
683 we showed that BDNF alone is not sufficient to induce new, fully functional synapses in
684 striatal neurons (Fig. 4). We presume that activity-dependent BDNF release by cortical
685 glutamatergic neurons activates TrkB receptors in striatal cells and turns on the
686 transcriptional programs instructing synapse formation (Hong et al., 2008). As a result, in
687 conjunction with neuronal activity, cortical input regulates the maintenance of those
688 synapses (Marty et al., 2000; Lin et al., 2008; West and Greenberg, 2011). To shed
689 further light on this mechanism future studies examining gene expression changes are
690 required.

691 To conclude, our study demonstrates the power of an *in vitro* approach to examine
692 inter-regional interactions between different neuronal types that are known to form
693 specific circuits *in vivo*. Using this two-neuron *in vitro* system, we were able to isolate
694 the specific role of glutamatergic innervation onto striatal GABAergic output, examine
695 specific parameters underlying synaptic function and study putative factors required for

696 glutamatergic-induced modulation. Nevertheless, to strengthen the relevance of our
697 findings, future studies examining striatal cell modulation *in vivo* are necessary.
698 Nowadays, that cumulative evidence support that basal ganglia circuit deficits are
699 implicated in numerous neurological diseases, including Huntington's disease (Cepeda et
700 al., 2003) and Tourette and Parkinson's syndromes , we are confident that our two-neuron
701 microcircuit model could be a valuable tool for assessing synaptic properties of such
702 disease models in cellular context. Understanding how cortical and thalamic inputs refine
703 striatal output will pave the way towards identifying basal ganglia activity in both
704 physiological and pathological conditions.
705
706 **References**

707 Albin RL, Young AB, Penney JB (1989) The functional anatomy of basal ganglia
708 disorder. Trends Neurosci 12:366–375.
709 Angevine JB, Sidman RL (1961) Autoradiographic study of cell migration during
710 histogenesis of cerebral cortex in the mouse. Nature 192:766–768.
711 Atallah B, Scanzianni M (2009) Instantaneous modulation of gamma oscillation
712 frequency by balancing excitation with inhibition. Neuron 62:566–577.
713 Barrows CM, McCabe MP, Chen H, Swann JW, Weston MC (2017) PTEN Loss
714 Increases the Connectivity of Fast Synaptic Motifs and Functional Connectivity in a
715 Developing Hippocampal Network. J Neurosci 37:8595–8611.
716 Baydyuk M, Xu B (2014) BDNF signaling and survival of striatal neurons. Front Cell
717 Neurosci 8:254.
718 Buren C, Tu G, Parsons MP, Sepers MD, Raymond LA (2016) Influence of cortical

719 synaptic input on striatal neuronal dendritic arborization and sensitivity to
720 excitotoxicity in corticostriatal co-culture. J Neurophysiol 116:380–390.
721 Cepeda C, Hurst RS, Calvert CR, Hernández-Echeagaray E, Nguyen OK, Jocoy E,
722 Christian LJ, Ariano MA, Levine MS, Herna E, Nguyen OK, Jocoy E, Christian LJ,
723 Ariano MA, Levine MS (2003) Transient and progressive electrophysiological
724 alterations in the corticostriatal pathway in a mouse model of Huntington's disease.
725 J Neurosci 23:961–969.
726 Chang C, Trimbuch T, Chao H, Jordan J, Herman MA, Rosenmund C (2014)
727 Investigation of Synapse Formation and Function in a Glutamatergic-GABAergic
728 Two-Neuron Microcircuit Chia-Ling. J Neurosci 34:855–868.
729 Cohen J (1988) Statistical power analysis for the behavioral sciences.
730 Conner JM, Lauterborn JC, Yan Q, Gall CM, Varon S (1997) Distribution of Brain-
731 Derived Neurotrophic Factor (BDNF) Protein and mRNA in the Normal Adult Rat
732 CNS: Evidence for Anterograde Axonal Transport. J Neurosci 17:2295–2313.
733 Cui G, Jun SB, Jin X, Pham MD, Vogel SS, Lovinger M, Costa RM (2013) Concurrent
734 Activation of Striatal Direct and Indirect Pathways During Action Initiation. Nature
735 494:238–242.
736 Czubayko U, Plenz D (2002) Fast synaptic transmission between striatal spiny projection
737 neurons. Proc Natl Acad Sci 99:15764–15769.
738 del Castillo BYJ, Katz B (1954) Quantal components of the end-plate potential. J Physiol
739 124:560–573.
740 DeLong MR (1990) Primate models of movement disorders of basal ganglia origin.
741 Trends Neurosci 13:281–285.

742 Ding J, Peterson JD, Surmeier DJ (2008) Corticostriatal and Thalamostriatal Synapses
743 Have Distinctive Properties. J Neurosci 28:6483–6492.
744 Doig NM, Moss J, Bolam JP (2010) Cortical and Thalamic Innervation of Direct and
745 Indirect Pathway Medium-Sized Spiny Neurons in Mouse Striatum. J Neurosci
746 30:14610–14618.
747 Fjodorova M, Noakes Z, Li M (2015) How to make striatal projection neurons.
748 Neurogenesis 2:1–6.
749 Fremeau RT, Troyer MD, Pahner I, Nygaard GO, Tran CH, Reimer RJ, Bellocchio EE,
750 Fortin D, Storm-mathisen J, Edwards RH (2001) The Expression of Vesicular
751 Glutamate Transporters Defines Two Classes of Excitatory Synapse. Neuron
752 31:247–260.
753 Fujiyama F, Furuta T, Kaneko T (2001) Immunocytochemical localization of candidates
754 for vesicular glutamate transporters in the rat cerebral cortex. J Comp Neurol
755 435:379–387.
756 Gerfen CR (1992) The neostriatal mosaic: multiple levels of compartmental organization.
757 Trends Neurosci 15:133–139.
758 Gharami K, Xie Y, An JJ, Tonegawa S, Xu B (2008) Brain-derived Neurotrophic Factor
759 Over-expression in the Forebrain Ameliorates Huntington's Disease Phenotypes in
760 Mice. J Neurochem 105:369–379.
761 Groenewegen HJ, Berendse HW (1994) The specificity of the "nonspecific" midline and
762 intralaminar thalamic nuclei. Trends Neurosci 17:52–57.
763 Hartman KN, Pal SK, Burrone J, Murthy VN (2006) Activity-dependent regulation of
764 inhibitory synaptic transmission in hippocampal neurons. Nat Neurosci 9:642–649.

765 Hong EJ, Mccord AE, Greenberg ME (2008) A biological function for the neuronal
766 activity-dependent component of Bdnf transcription in the development of cortical
767 inhibition. Neuron 60:610–624.
768 Huang ZJ, Kirkwood A, Pizzorusso T, Porciatti V, Morales B, Bear MF, Maffei L,
769 Tonegawa S (1999) BDNF regulates the maturation of inhibition and the critical
770 period of plasticity in mouse visual cortex. Cell 98:739–755.
771 Kemp JM, Powell TPS (1970) The cortico-striate projection in the monkey. Brain
772 93:525–546.
773 Kolodziejczyk K, Raymond LA (2016) Differential changes in thalamic and cortical
774 excitatory synapses onto striatal spiny projection neurons in a Huntington disease
775 mouse model. Neurobiol Dis 86:62–74.
776 Kreitzer AC, Malenka RC (2008) Striatal plasticity and basal ganglia circuit function.
777 Neuron 60:543–554.
778 Lin Y, Bloodgood BL, Hauser JL, Lapan AD, Koon AC, Kim T, Hu LS, Malik AN,
779 Greenberg ME (2008) Activity-dependent regulation of inhibitory synapse
780 development by Npas4. Nature 455:1198–1204.
781 Liu G (2004) Local structural balance and functional interaction of excitatory and
782 inhibitory synapses in hippocampal dendrites. Nat Neurosci 7:373–379.
783 Liu H, Chapman ER, Dean C (2013) “Self” versus “Non-Self” Connectivity Dictates
784 Properties of Synaptic Transmission and Plasticity. PLoS One 8:1–9.
785 Liu H, Dean C, Arthur CP, Dong M, Chapman ER (2009) Autapses and Networks of
786 Hippocampal Neurons Exhibit Distinct Synaptic Transmission Phenotypes in the
787 Absence of Synaptotagmin I. J Neurosci 29:7395–7403.

788 Marty S, Wehrlé R, Sotelo C (2000) Neuronal activity and brain-derived neurotrophic
789 factor regulate the density of inhibitory synapses in organotypic slice cultures of
790 postnatal hippocampus. J Neurosci 20:8087–8095.
791 McGeorge AJ, Faull RLM (1989) The organization of the projection from the cerebral
792 cortex to the striatum in the rat. Neuroscience 29:503–537.
793 Meijering E, Jacob M, Sarria JF, Steiner P, Hirling H, Unser M (2004) Design and
794 Validation of a Tool for Neurite Tracing and Analysis in Fluorescence Microscopy
795 Images. Cytometry 58:167–176.
796 Nakao N, Brundin P, Funa K, Lindvall O, Odin P (1995) Trophic and protective actions
797 of brain-derived neurotrophic factor on striatal DARPP-32-containing neurons in
798 vitro. Dev Brain Res 90:92–101.
799 Oldenburg IA, Sabatini BL (2015) Antagonistic but not symmetric regulation of primary
800 motor cortex by basal ganglia direct and indirect pathways. Neuron 86:1174–1181.
801 Palizvan MR, Sohya K, Kohara K, Maruyama A, Yasuda H, Kimura F, Tsumoto T
802 (2004) Brain-derived neurotrophic factor increases inhibitory synapses, revealed in
803 solitary neurons cultured from rat visual cortex. Neuroscience 126:955–966.
804 Park H, Poo MM (2013) Neurotrophin regulation of neural circuit development and
805 function. Nat Rev Neurosci 14:7–23.
806 Penrod RD, Campagna J, Panneck T, Preese L, Lanier LM (2015) The presence of
807 cortical neurons in striatal-cortical co-cultures alters the effects of dopamine and
808 BDNF on medium spiny neuron dendritic development. Front Cell Neurosci 9:1–14.
809 Randall FE, Garcia-Munoz M, Vickers C, Schock SC, Staines WA, Arbuthnott GW
810 (2011) The Corticostriatal System in Dissociated Cell Culture. Front Syst Neurosci

811 5:1–7.
812 Rauskolb S, Zagrebelsky M, Dreznjak A, Deogracias R, Matsumoto T, Wiese S, Erne B,
813 Sendtner M, Schaeren-Wiemers N, Korte M, Barde Y-A (2010) Global Deprivation
814 of Brain-Derived Neurotrophic Factor in the CNS Reveals an Area-Specific
815 Requirement for Dendritic Growth. J Neurosci 30:1739–1749.
816 Reim K, Mansour M, Varoqueaux F, McMahon HT, Südhof TC, Brose N, Rosenmund C
817 (2001) Complexins regulate a late step in Ca2+-dependent neurotransmitter release.
818 Cell 104:71–81.
819 Rosenmund C, Stevens CF, Zellula AG (1996) Definition of the Readily Releasable Pool
820 of Vesicles at Hippocampal Synapses. Neuron 16:1197–1207.
821 Rothwell P, Hayton SJ, Sun GL, Fuccillo M V, Hopkins K, Kook Lim B, Malenka RC
822 (2015) Input- and Output-Specific Regulation of Serial Order Performance by
823 Corticostriatal Circuits. Neuron 88:345–356.
824 Salin P, Kachidian P (1998) Thalamo-striatal deafferentation affects preproenkephalin
825 but not preprotachykinin gene expression in the rat striatum. Mol Brain Res 57:257–
826 265.
827 Sciamanna G, Ponterio G, Mandolesi G, Bonsi P, Pisani A (2015) Optogenetic
828 stimulation reveals distinct modulatory properties of thalamostriatal vs
829 corticostriatal glutamatergic inputs to fast-spiking interneurons. Sci Rep 5:1–15.
830 Segal M, Greenberger V, Korkotian E (2003) Formation of dendritic spines in cultured
831 striatal neurons depends on excitatory afferent activity. Eur J Neurosci 17:2573–
832 2585.
833 Smeal RM, Gaspar RC, Keefe KA, Wilcox KS (2007) A rat brain slice preparation for

characterizing both thalamostriatal and corticostriatal afferents. J Neurosci Methods 159:224–235.

Smith AD, Bolam JP (1990) The neural network of the basal ganglia as revealed by the study of synaptic connections of identical neurones. Trends Neurosci 13:259–265.

Smith Y, Raju D V, Pare JF, Sidibe M (2004) The thalamostriatal system: A highly specific network of the basal ganglia circuitry. Trends Neurosci 27:520–527.

Stern E a, Kincaid a E, Wilson CJ (1997) Spontaneous subthreshold membrane potential fluctuations and action potential variability of rat corticostriatal and striatal neurons in vivo. J Neurophysiol 77:1697–1715.

Taverna S, Ilijic E, Surmeier DJ (2008) Recurrent collateral connections of striatal medium spiny neurons are disrupted in models of Parkinson's disease. J Neurosci 28:5504–5512.

Tunstall MJ, Oorschot DE, Kean A, Wickens JR (2002) Inhibitory Interactions Between Spiny Projection Neurons in the Rat Striatum. J Neurophysiol 88:1263–1269.

West AE, Greenberg ME (2011) Neuronal Activity – Regulated Gene Transcription in Synapse Development and Cognitive Function. Cold Spring Harb Perspect Biol 3:1–21.

Wichterle H, García-Verdugo JM, Alvarez-Buylla A (1997) Direct evidence for homotypic, glia-independent neuronal migration. Neuron 18:779–791.

Wilson CJ (1993) The generation of natural firing patterns in neostiatal neurons. Prog Brain Res 99:277–297.

Wilson CJ (2014) The Sensory Striatum. Neuron 83:999–1001.

Figure legends

Figure 1. Striatal GABAergic output is modulated by glutamatergic input. (A-C) Schematic diagram illustrating autaptic and heterosynaptic connections in striatal (GABAergic only; dark blue), cortico-striatal (glu-GABA; pink) and thalamo-striatal (glu-GABA; green) pairs. (D-Q) Functional analysis of striatal autapses (light blue traces and dots), striatal pairs (blue traces and dark blue dots), cortico-striatal pairs (pink traces and dots) and thalamo-striatal pairs (green traces and dots). (D-F) Representative traces of GABAergic response to paired pulse stimulation with 50 ms inter-stimulus interval and to a five second pulse of 500 mM hypertonic sucrose solution (dark; autaptic, light; heterosynaptic). (G-J) Scatter plots showing total evoked IPSC amplitudes (G), RRP size (H), Pvr% (I) and PPR (J). (K-M) Representative traces showing miniature postsynaptic current activity (dark; autaptic, light; heterosynaptic). (N-Q) Scatter plots showing mean mIPSC amplitudes (N), charge (O), frequency (P), and RRP vesicles number (Q). (R) Representative traces of glutamatergic response to paired pulse stimulation with 25 ms inter-stimulus interval (dark; autaptic, light; heterosynaptic, pink; cortico-striatal pairs, green; thalamo-striatal pairs). (S-T) Scatter plots showing total evoked EPSC amplitudes (S) and PPR (T). (U-V) Bars graphs showing the mean PSC amplitude of autaptic and heterosynaptic responses of glutamatergic (U) and GABAergic neurons in homotypic or heterotypic pairs (V). Data shown as mean ± SEM. * refers to $p \leq 0.05$, ** $p \leq 0.01$ and *** $p \leq 0.001$. See also Extended Data Table Figure 1-1.

Figure 2. Cortical input increases the number of GABAergic synapses in striatal neurons. (A-B) Morphological analysis of striatal autapses (light blue dots), striatal pairs

(dark blue dots), cortico-striatal pairs (pink dots) and thalamo-striatal pairs (green dots). (A) Representative images of neuronal morphology showing immunoreactivity for MAP2, VGAT and VGLUT1 (cortical synapses) or VGLUT2 (thalamic synapses). (B-C) Scatter plots showing the number of VGAT synapses per neuron (B), the number of VGLUT1 or VGLUT2 synapses per neuron (C) and mean membrane capacitance measurements as obtained from the membrane test (D). Data shown as mean ± SEM. * refers to $p \leq 0.05$, ** $p \leq 0.01$, *** $p \leq 0.001$ and **** $p \leq 0.0001$. See also Extended Data Table Figure 2-1.

Figure 3. Activity modulates GABAergic synapse output in cortico-striatal pairs. (A-F) Functional analysis of striatal pairs (blue color scale dots), cortico-striatal pairs (red color scale dots). Scatter plots showing total evoked IPSC amplitudes (A), RRP size (B), Pvr% (C), mIPSC amplitudes (D), RRP vesicles number (E) and mean membrane capacitance measurements as obtained from the membrane test (F). Data shown as mean ± SEM. * refers to $p \leq 0.05$, ** $p \leq 0.01$, *** $p \leq 0.001$ and **** $p \leq 0.0001$. See also Extended Data Table Figure 3-1.

Figure 4. Exogenous BDNF promotes growth and synapse formation in striatal autaptic neurons. (A-D) Morphological analysis of striatal autapses (control; light blue, BDNF treated; yellow, Trk-antagonist treated; purple, BDNF and Trk-antagonist treated; green). (A) Representative images of neuronal morphology showing immunoreactivity for MAP2 and VGAT. (B-D) Scatter plots showing neuronal soma area (B), number of VGAT synapses per neuron (C) and mean total dendritic length (D). (E-L) Bar graphs

showing evoked IPSC amplitudes (E), RRP size (F), PPR (G), mean mIPSC amplitudes (H), frequency (J), RRP vesicles number (I), (K) normalized response amplitude to 5μM GABA and membrane capacitance (L). Data shown as mean ± SEM. * refers to $p \leq 0.05$, ** $p \leq 0.01$ and *** $p \leq 0.001$. See also Extended Data Table Figure 4-1.

Figure 5. BDNF release modulates GABAergic synapse output in cortico-striatal pairs. (A) Bar graph showing real-time RT-PCR analysis for mRNA expression of *Bdnf* gene in striatal and cortical neuronal mass cultures. (B-H) Functional analysis of striatal pairs (untreated; dark blue, Trk-antagonist treated; purple), cortico-striatal pairs (untreated; pink, Trk-antagonist treated; brown). Scatter plots showing mean evoked IPSC amplitudes (B), RRP size (C), PPR (D), mIPSC amplitudes (E), mIPSC frequency (F), RRP vesicles number (G) and mean membrane capacitance measurements as obtained from the membrane test (H). (J-K) Representative images of neuronal morphology showing immunoreactivity for MAP2, VGAT and VGLUT1. Scatter plots showing the number of VGAT synapses per neuron (I), the number of VGLUT1 synapses per neuron (K). Data shown as mean ± SEM. * refers to $p \leq 0.05$, ** $p \leq 0.01$, *** $p \leq 0.001$ and **** $p \leq 0.0001$. See also Extended Data Table Figure 5-1.

Extended data

Figure 1-1. Descriptive statistics and pairwise comparisons between groups for Figure 1. Data shown as mean ± SEM. For statistics: H refers to Kruskal-Wallis test, U refers to Mann-Whitney test and t refers to Student's t test.

	striat aut	striat+striat	striat+cortex	striat+thal	Statistics	P-value
IPSC amp. (nA)	-7.63±1.19	-10.51± 1.23	-21.14±3.12	-19.13±3.29	H(3,159)=26.29	<0.0001
RRP charge (nC)	-3.18±0.35	-3.77±0.30	-6.30±0.62	-7.61±0.91	H(3,149)=32.68	<0.0001
Pvr (%)	13.63±1.56	13.66±1.24	11.64±1.79	14.07±1.76	H(3,143)=2.14	0.5433
PPR (50ms)	0.71±0.07	0.86±0.08	0.72±0.08	0.89±0.14	H(3,135)=3.36	0.3389
mIPSC amp. (pA)	-42.42±3.71	-44.31±3.04	-74.24±7.07	-79.17±8.16	H(3,157)=29.93	<0.0001
mIPSC charge (fC)	-742.10±71.86	-838.10±68.96	-1379±129.2	-1454±172.5	H(3,157)=26.40	<0.0001
mIPSC freq. (Hz)	2.22±0.34	2.15±0.26	1.70±0.35	2.54±0.47	H(3,164)=4.97	0.1736
#RRP vesicles	5738±728.2	4445±362	8498±1700	5197±990	H(3,95)=6.381	0.0945
EPSC amp. (nA)	-	-	-9.78±1.53	-4.72±0.95	U =214	0.006
glu PPR (25ms)	-	-	0.98±0.05	1.06±0.09	t(53)=0.81	0.4187

Figure 2-1. Descriptive statistics and pairwise comparisons between groups for Figure 2. Data shown as mean ± SEM. For statistics: H refers to Kruskal-Wallis test and U refers to Mann-Whitney test.

	striat aut	striat+striat	striat+cortex	striat+thal	Statistics	P-value
VGAT synapses	184±22.07	174.8±17.48	326.3±41.52	175.4±17.72	H(3,94)= 12.7	0.0053
VGLUT1/2synapses			312.2±38.7	118.2±15.5	U= 74	<0.0001
Cm (pF)	17.23±1.47	20.22±1.32	24.75±2.32	24.02±2.87	H(3,157)=10.35	0.0158

Figure 3-1. Descriptive statistics and pairwise comparisons between groups for Figure 3. Data shown as mean ± SEM. For statistics: H refers to Kruskal-Wallis test.

	striat+striat	striat+striat +TTX	striat+striat +NBQX/APV	striat+cortex	striat+cortex +TTX	striat+cortex +NBQX/APV	Statistics	P-value
IPSC amp. (nA)	-5.74±0.91	-8.84±1.51	-6.04±1.36	-17.93±1.87	-7.34±1.25	-7.50±0.89	H(5,160)=37.77	<0.0001
RRP charge (nC)	-2.18±0.25	-2.69±0.27	-3.19±0.58	-6.75±0.67	-3.88±0.66	-3.39±0.58	H(5,158)=43.24	<0.0001
Pvr (%)	15.77±1.55	20±2.45	15.26±2.99	13.98±1.55	14.86±2.39	15.12±1.40	H(5,153)=5.18	0.3943
PPR (50ms)	0.74±0.07	0.72±0.09	0.92±0.11	0.65±0.05	0.56±0.06	0.63±0.08	H(5,162)=6.92	0.2268
mIPSC amp. (pA)	-55.15±4.28	-62.78±3.82	-62.4±4.83	-77.56±4.51	-50.61±4.23	-54.62±5.15	H(5,239)=25.42	0.0001
mIPSC charge (fC)	-1024±83.57	-1187±97.22	-1231±136.4	-1529±110.5	-938.6±103.6	-896.5±114.3	H(5,240)=23.81	0.0002
mIPSC freq. (Hz)	1.443±0.33	1.971±0.35	1.43±0.46	1.171±0.17	1.403±0.32	1.177±0.33	H(5,261)=6.82	0.2343
#RRP vesicles	2740±450.7	3875±693.5	3163±611.7	5988±716.1	2963±451.9	2837±388.6	H(5,152)=17.84	0.0032
Cm (pF)	19.3±1.24	19.06±1.19	19.11±1.59	27.11±2.85	17.5±1.87	21.53±2.12	H(5,169)= 6.67	0.2464

Figure 4-1. Descriptive statistics and pairwise comparisons between groups for Figure 4 plots A-D (A) and plots E-L (B). Data shown as mean ± SEM. For statistics: H refers to Kruskal-Wallis test, U refers to Mann-Whitney test and t refers to Student's t test.

A	striat aut	striat+BDNF	striat+K252a	striat+BDNF +K252a	Statistics	P-value
Soma size (μm^2)	92.66±5.47	168.1±9.21	108.6±11.42	122.9±6.80	H(3,148)= 39.84	<0.0001
VGAT synapses	127.6±14	238.5±20.03	103.8±14.7	120.3±10.72	H(3,144)=30.45	<0.0001
Dendritic length (µm)	714.3±62.08	1251±93.45	762.5±89.26	783.7±73.33	H(3,151)=25.2	<0.0001

B	Control	BDNF	Statistics*	P-value
IPSC amp. (nA)	-6.84±0.63	-5.89±0.63	U=3818	0.0126
RRP charge (nC)	-3.13±0.29	-2.47±0.17	U=4143	0.0921
Pvr (%)	13.19±1.03	10.74±0.81	U=3725	0.0081
PPR (50ms)	0.72±0.04	0.79±0.04	U=4049	0.2182
mIPSC amp. (pA)	-50.12±2.87	-39.27±1.88	U=3190	0.0009
mIPSC charge (fC)	-823.9±55.53	-660±37.47	U=3462	0.0132
mIPSC freq. (Hz)	1.55±0.26	1.79±0.19	U=3769	0.05
# RRP vesicles	4663±464.7	4542±327.6	U=4724	0.9248
Cm (pF)	17.78±1.06	21.69±0.90	U=3511	0.0005
GABA current	1±0.1	0.97±0.09	t(16)=0.21	0.8345

Figure 5-1. Descriptive statistics and pairwise comparisons between groups for Figure 5 plots B-H (A) and plots I-K (B). Data shown as mean ± SEM. For statistics: H refers to Kruskal-Wallis test and U refers to Mann-Whitney test.

A	striat+striat	striat+cortex	striat+striat +K252a	striat+cortex +K252a	Statistics	P-value
IPSC amp. (nA)	-5.21±0.89	-10.38±1.23	-5.55±0.87	-7.73±1.47	H(3,169)=12.72	0.0053
RRP charge (nC)	-2.29±0.26	-4.58±0.37	-1.77±0.16	-2.74±0.38	H(3,155)=38.67	<0.0001
Pvr (%)	10.68±1.1	8.36±0.77	14.07±1.44	12.92±2.29	H(3,152)=9.95	0.019
PPR (50ms)	1.03±0.10	0.95±0.09	0.10±0.13	0.96±0.12	H(3,168)=1.50	0.6829
mIPSC amp. (pA)	-42.96±2.58	-66.59±4.64	-37.71±3.62	-46.82±3.55	H(3,203)=26.46	<0.0001
mIPSC charge (fC)	-728.6±60.4	-1182±82.97	-596.2±53.31	-866±72.94	H(3,202)=26.66	<0.0001
mIPSC freq. (Hz)	1.89±0.24	1.21±0.18	1.42±0.23	1.32±0.22	H(3,210)=11.55	0.0091
# RRP vesicles	3364±452.8	5846±605.6	3147±321.2	4136±724.9	H(3,149)=13.68	0.0034
Cm (pF)	15.67±1.12	22.45±2.09	19.39±1.39	16.85±1.14	H(3,170)=5.63	0.1309

B	striat+striat	striat+cortex	striat+cortex +anti-BDNF	striat+cortex +K252a	Statistics	P-value
VGAT synapses	216.9±18.41	498.5±63.2	197.7±22.99	269.3±30.89	H(3,130)= 12.7	0.0053
VGLUT1 synapses		570.6±52.46	314.8±29.01	377.5±45.63	H(2,95)= 13.45	0.0012

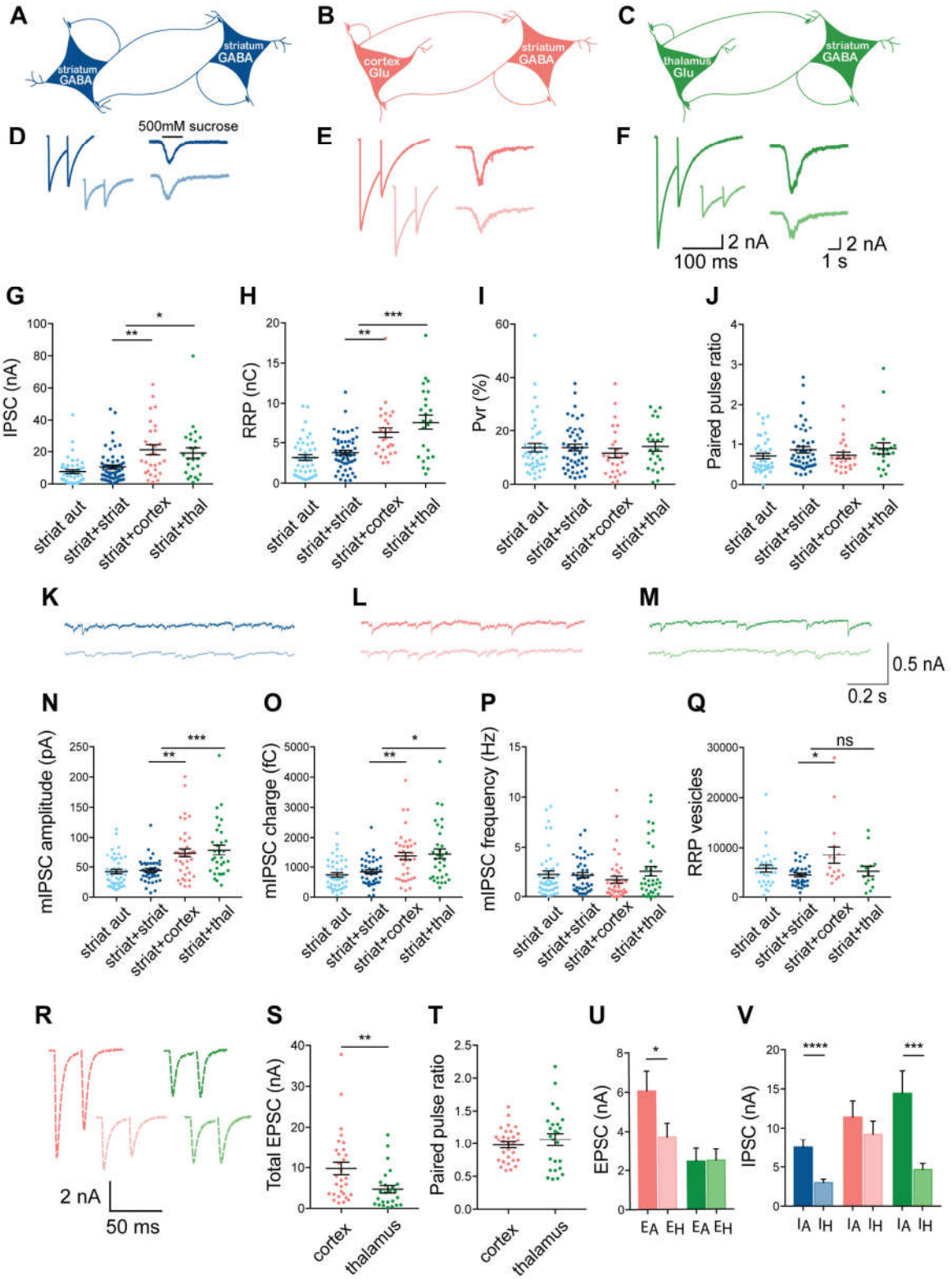

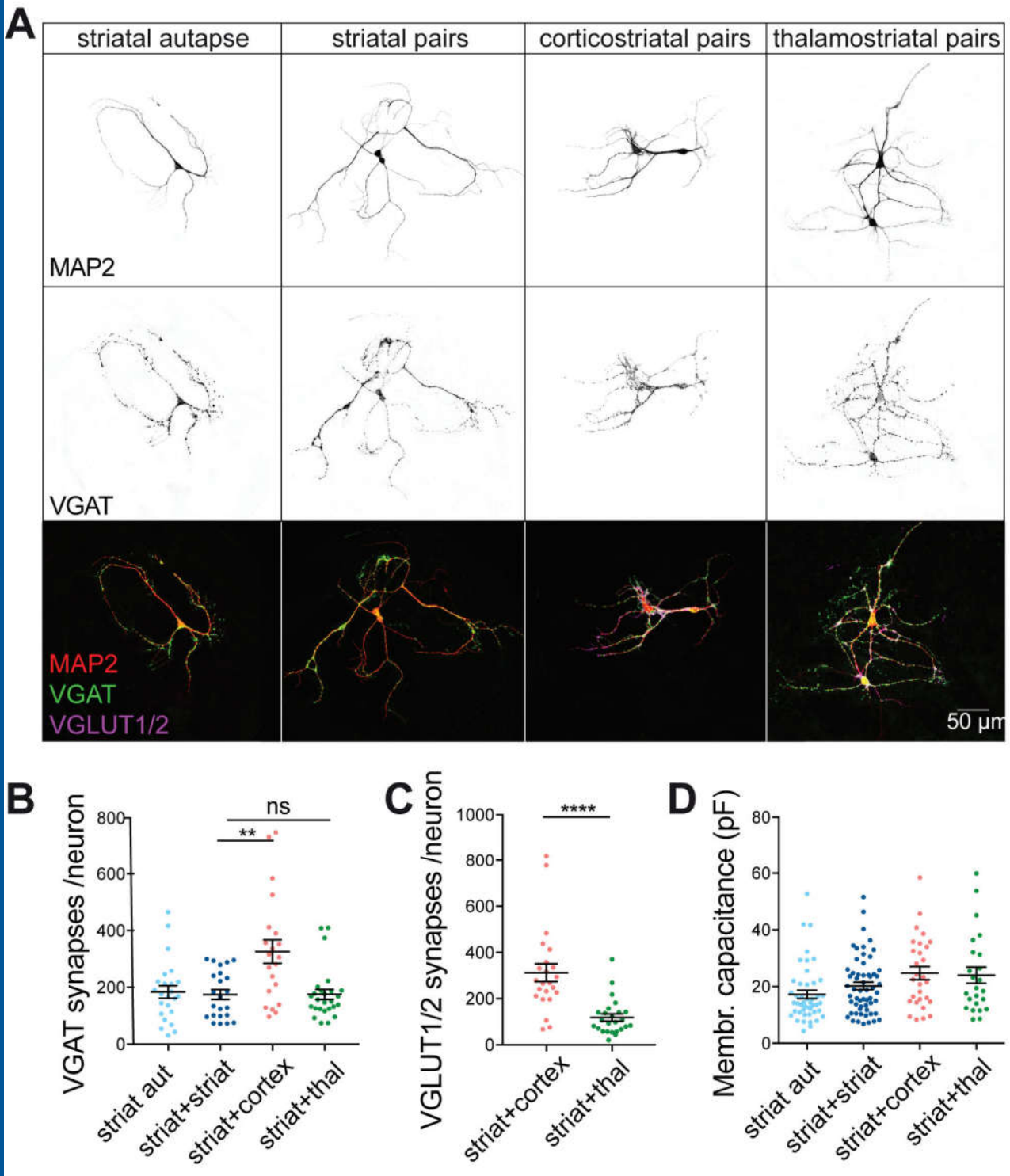

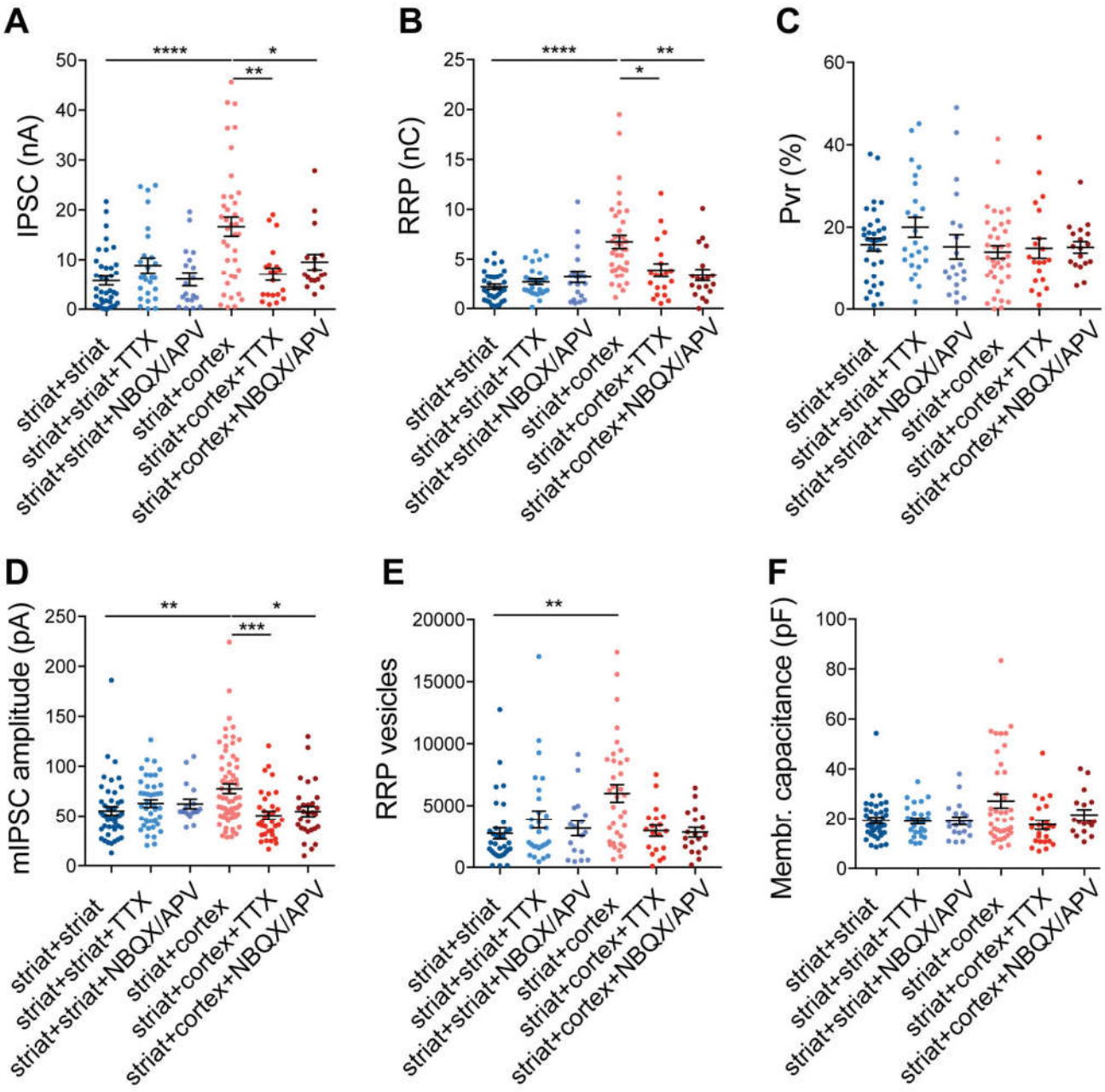

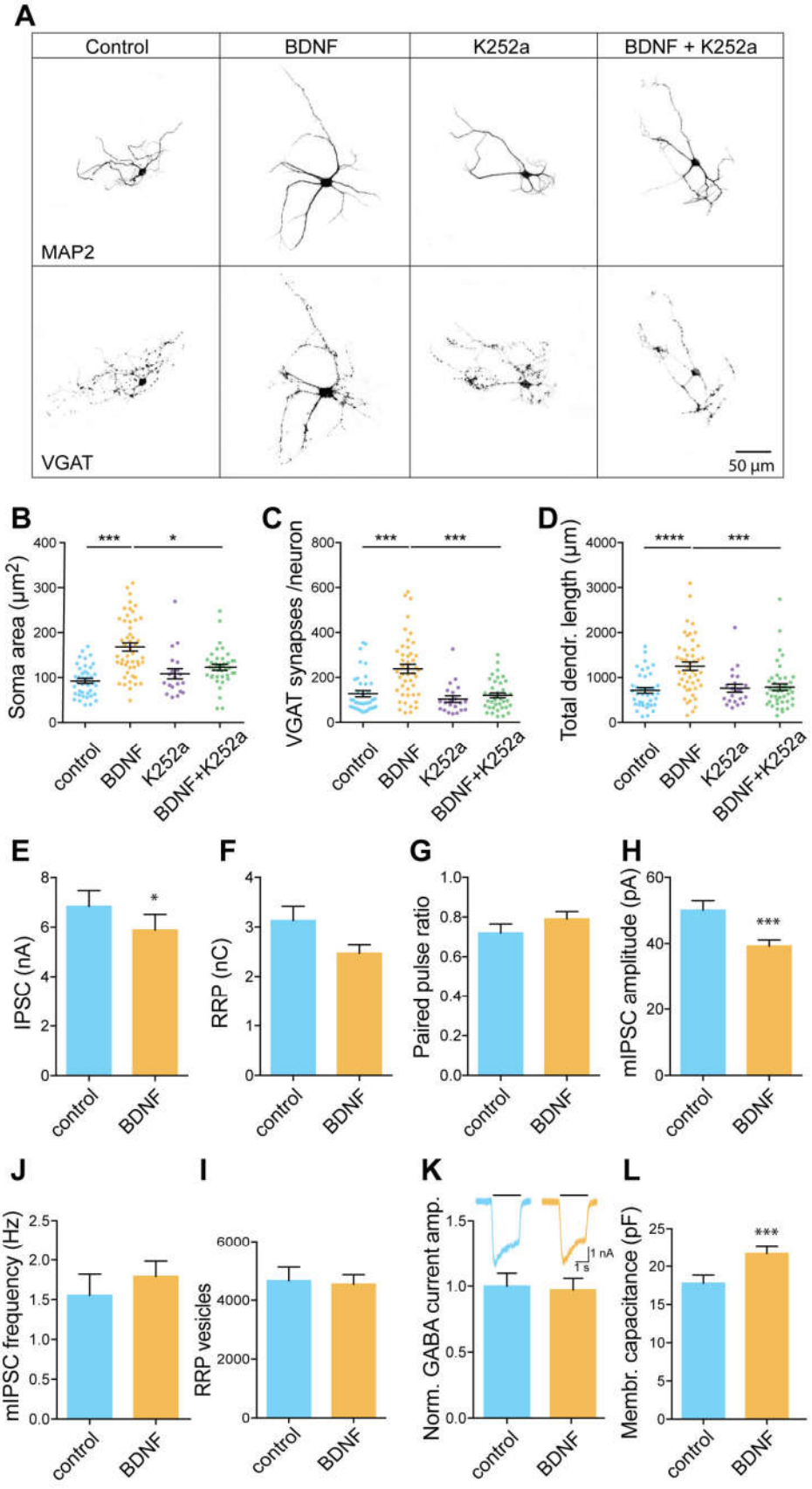

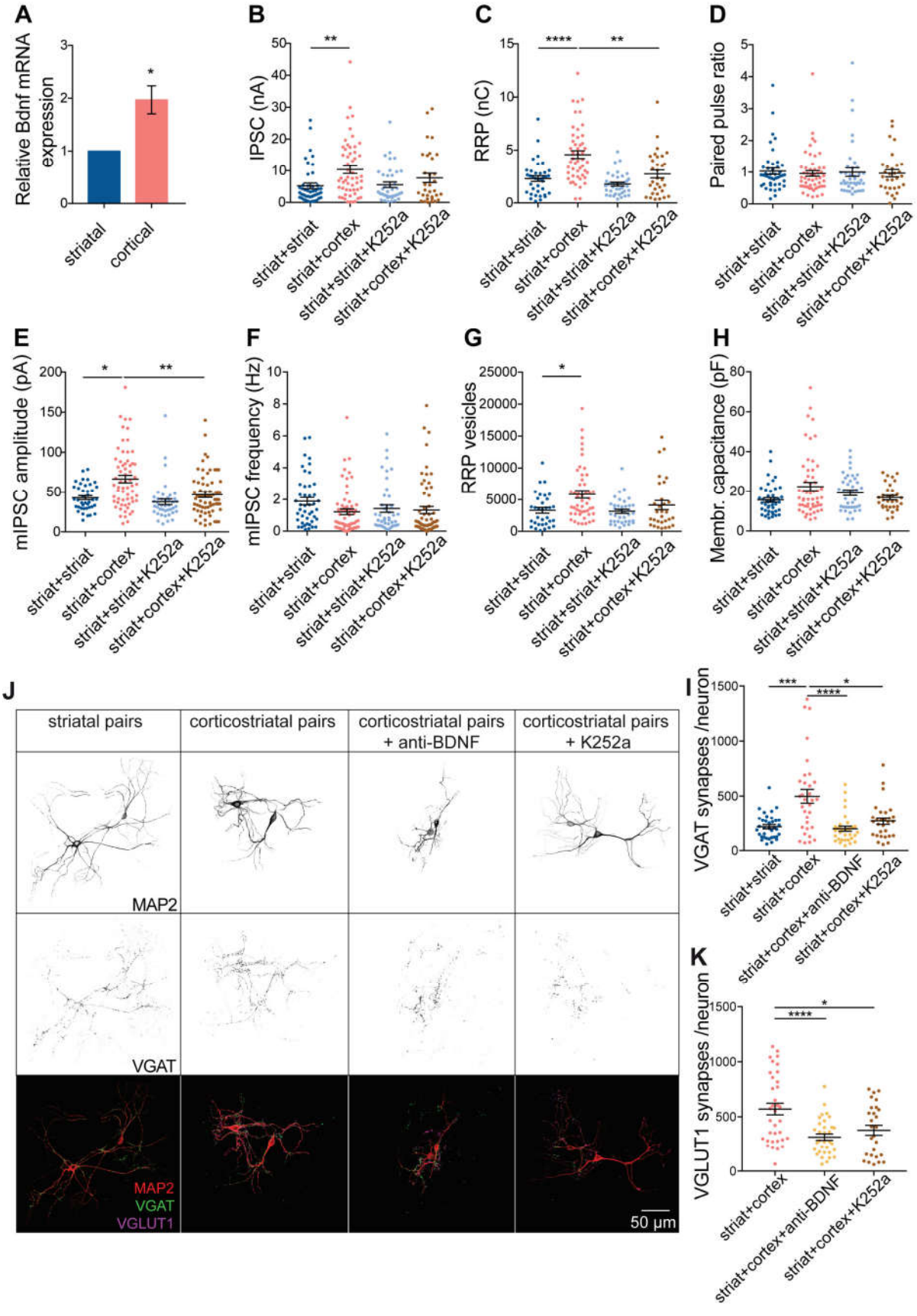

My curriculum vitae does not appear in the electronic version of my paper for reasons of data protection.

My curriculum vitae does not appear in the electronic version of my paper for reasons of data protection.

My curriculum vitae does not appear in the electronic version of my paper for reasons of data protection.

Complete list of publications

1. **Paraskevopoulou, F.**, Herman, M.A., Rosenmund, C. (2019). Glutamatergic innervation onto striatal neurons potentiates GABAergic synaptic output. *Journal of Neuroscience*, 10.1523/JNEUROSCI.2630-18.2019 (Impact factor 5.971)

2. Papadopoulos, T., Rhee, H. J., Subramanian, D., **Paraskevopoulou, F.**, Mueller, R., Schultz, C., et al. (2016). Endosomal Phosphatidylinositol 3-Phosphate Promotes Gephyrin Clustering and GABAergic Neurotransmission at Inhibitory Postsynapses. *Journal of Biological Chemistry*, 292(4), 1160-1177, doi:10.1074/jbc.m116.771592 (Impact factor 4.010)

Acknowledgments

I would like to express my gratitude to my doctoral supervisor Christian Rosenmund for giving me the opportunity to be part of his lab and encouraging me to try out novel and risky projects. I want to thank him for his constant support, guidance and mentoring throughout all the phases of my PhD.

Together with Christian, Melissa Herman has always been there to advise and co-supervise me. I would like to thank her deeply for her patience and support during all these years, as well as for inspiring me and shaping me as a scientist.

I would also like to address my gratitude to my co-supervisor Ferah Yildirim for all her scientific advise in the single-cell RNA seq projects. I want to thank her for being so supportive, for strongly believe in me and for trusting me to be part of her amazing team. I truly enjoyed working with her and having all those discussions both about science and life.

I would also like to thank all of my colleagues and friends in Rosenmund lab for their support and useful input during our countless lab meetings. Special thanks to my dearest friends, Fereshteh Zarebidaki and Mayur Vadhvani, for standing next to me and for offering their warm hug.

A sincere thank you also goes to all the technicians in Rosenmund lab for their valuable technical support.

I feel indebted to MedNeuro PhD program for offering me the opportunity to participate in their program and its accompanying courses and scientific retreats which have all offered me useful soft skills and a valuable environment of interactions with other scientists. I would also like to address my gratitude to NeuroCure Cluster of Excellence for financially supporting me during the first years of my PhD.

I would also like to thank all of my closest friends, Athanasia Drakoulia, Evangelia Giannakopoulou, Lena Siouti, Maria Katsantoni, who have always believed in me and supported me in the most difficult times. I thank them for their unconditional love and for always being there.

My family – my parents and my brother – deserve a big thank you for always having my back, believe in me and support me in all possible ways.

Last but not least, I would like to thank my life partner Kostas Sagonas for his unconditional love and endless patience, for always being on my side and smiling.